The Influence of Timing on the Hemodynamic Effects of Compression Devices and Development of Sensor Driven Timing Mechanisms

by

Allie Fawcett

A thesis

presented to the University of Waterloo

in fulfilment of the

thesis requirement for the degree of

Master of Applied Science

in

Mechanical and Mechatronics Engineering

Waterloo, Ontario, Canada, 2018

Author's declaration

This thesis consists of material all of which I authored or co-authored: see Statement of Contributions included in the thesis. This is a true copy of the thesis, including any required final revisions, as accepted by my examiners.

I understand that my thesis may be made electronically available to the public.

Statement of Contributions

The author contributions are detailed below.

Chapter 2: Kathryn A. Zuj, Chekema N. Prince, Richard L. Hughson and Sean D. Peterson aided me in the conception of the design of the research. Kathryn A. Zuj helped me with the data collection of the study. I completed the initial draft of the chapter. Chekema N. Prince and Sean D. Peterson contributed to the editing of this chapter.

Chapter 3: Chekema N. Prince, Richard L. Hughson and Sean D. Peterson aided me in the conception of the design of the research. I completed the initial draft of the chapter. Chekema N. Prince and Sean D. Peterson contributed to the editing of this chapter.

Abstract

Long periods of reduced mobility are associated with formation of blood clots in the deep veins of the legs, referred to as deep vein thrombosis (DVT). DVT has been noted as a large factor of morbidity and mortality in clinical settings as the clots can move from the legs to the lungs causing blockages, known as pulmonary embolisms. Preventing venous stasis has been clinically linked to preventing DVT formation. Venous stasis can be prevented by applying active mechanical compressions to the lower limbs, such as with an intermittent pneumatic compression (IPC) device; these devices have been clinically shown to reduce venous stasis and thereby prevent DVT formation. The main objectives of this thesis were to assess and improve a custom cardiac gated compression (CGC) system that times compressions based on an individual's heartrate so as to only apply compressions during the diastolic phase of the cardiac cycle.

A comparative performance assessment was done by measuring the central and peripheral hemodynamic changes induced by the use of different IPC devices (ArjoHuntleigh Flowtron ACS800 (Flowtron), Kendall SCD Express (SCD), Aircast Venaflow Elite (VenaFlow), and the custom CGC system) on 12 healthy human subjects in both seated and supine positions. The four selected compression devices had similar applied pressure levels, but dramatically different application profiles with regards to timing and method of application (e.g., single uniform bladder versus sequential inflation from ankle to knee). In addition, the compression systems were delineated by "smart" versus fixed timing, with two devices employing physiological measures to adjust when compression occurred (SCD: slow inflation based on vascular refill time; CGC: rapid inflation based on cardiac gating), and two inflating at fixed intervals (VenaFlow: rapid inflation; Flowtron: slow inflation). The devices were tested for ten minutes while heart rate, stroke volume, cardiac output, calf muscle oxygenation, and femoral venous and superficial femoral arterial velocities measures were collected. From the femoral venous velocities, the velocity per minute, peak velocity during the compression period, and the displacement per compression and per hour were used as performance metrics.

With respect to the peak velocity the VenaFlow resulted in higher results than all other devices; likely due to its rapid inflation characteristics and the frequency of compressions allowing pooling to occur in the legs. However, in the performance metric of average displacement per compression the Flowtron and SCD resulted in the greatest displacements; likely because of the devices' longer inflation periods resulting in a longer increase in venous velocity per compression. However, this

measure does not account for the frequency of compressions unlike the displacement per hour measurement; the displacement of venous blood per hour resulted in the CGC device performing as well as the slow inflation devices during supine and resulted in greater displacement than all other devices in the seated position. The CGC also resulted in a sustained increase on the systemic and peripheral hemodynamics in the measures of SV when seated, and arterial velocity and muscle oxygenation when seated and supine; this can potentially be attributed to the device's cardiac gating and resultant compression frequency. Interestedly, the Flowtron and SCD's behaviour in most measures taken at steady state were not significantly different despite the "smart" timing employed by the SCD.

The current timing mechanism of the CGC device is based on the previous R-R interval of the electrocardiograph (ECG) trace and a fixed pulse wave transit time. Due to heart rate variability and changes in vascular conductance, the compressions of the CGC could be more reliably triggered based on a local measurement of the pulse arrival. To address this need, a custom pulse sensor that uses photoplethysmography (PPG) to detect the pulse in the lower limb was developed. Key problems that impact wearable PPG sensor performance are motion, the power requirements of the LEDs and the ability to work on darker skin pigmentations.

The sensor design was done with the primary objective of reliably and robustly detecting the pulse wave arrival regardless of skin tone or application location, and the secondary objective of maximizing the battery life of the sensor for future potential applications in wearable technologies. The developed sensor is reflectance-based and employs 6 independently controlled light emitting diodes (LEDs) surrounding a single photodiode. The independent control enables the "best" LED configuration to be selected through an in situ calibration cycle that results in the strongest signal at the lowest power setting required for different skin pigmentations in non-motion and motion conditions. The shin, in comparison to the foot and ankle, was determined as the best measurement location in terms of motion resistance and low power requirements. Furthermore, the calibration cycle proved to effectively adapt to the underlying physiology and find the LED configuration that resulted in the strongest pulse signal at the lowest possible power setting for each individual. Therefore, as the PPG sensor was proven to work effectively from the lower limb, further improvement to the timing of compressions for the CGC device may be possible through the integration of the peripheral pulse detection sensor.

Acknowledgements

First and foremost, Sean Peterson and Chekema Prince, thank you for your guidance, patience and for pushing me to be a better researcher; your mentorship has been invaluable. Thank you to Richard Hughson, for providing key insights and guidance in understanding the effects of the physiology on my research.

Thank you to everyone on the SHP team, you all provided me with key insights and helped me to reach higher levels with my research. Kathryn Zuj, thank you so much for helping me with data collection and for your endless patience when you answered all my physiology-based questions as I realized that the human body was not going to behave like a machine.

Thank you to my friends and family, for supporting me through every moment of this insanity.

Thanks to all of my study participants for offering your time for my research. Special thanks to Neil Griffett, who helped with soldering and fabricated the PCBs for my sensors. And finally, thank you Joslin Goh and Yidan Shi, for answering my endless statistics questions.

Table of Contents

List of Figures

List of Tables

Chapter 1

1.1 Introduction and Background

Venous thromboembolism (VTE) is a vascular disease that is made up of two components, deep vein thrombosis (DVT) and pulmonary embolisms (PE) [1], [2]. DVT occurs when blood clots form in the deep veins of the leg [3], [4]. PE is primarily the result of clots moving from the deep veins of the legs to the lungs, which can cause blockages in the lungs and is a major cause of morbidity and mortality in intensive care units [4], [5]; 10% of all PE cases are fatal within the first hour of symptoms appearing for the patient [4], [5]. DVT prevention is key to reducing subsequent complications and the incidence of fatalities.

Prevention treatments aim to address one or more of Virchow's triad of factors (i.e. venous stasis, vessel damage, and hypercoagulability) that cause DVT [6]–[10]. Based on clinical results, hospitalized patients, particularly post-surgical patients, have a higher risk for DVT due to venous stasis exacerbated by their reduced mobility [1], [7], [11]–[13]. The risk of DVT increases with both age and the length of the surgery [14]. It is estimated that 20% of patients that undergo a major surgical procedure will develop DVT; however, in patients that undergo orthopedic surgery the risk of DVT is particularly prevalent, as an estimated 40% will develop DVT [15].

There are two broadly classified preventative treatments for DVT; pharmacological solutions, typically in the form of anti-coagulants, and external prophylaxes that encourage venous flow through mechanical limb compression. External compression can be applied with intermittent pneumatic compression (IPC) devices which have been proven to effectively lower the risk of DVT formation [6], [9]–[11], [15]–[18], while also having a lower associated risk of bleeding

complications than pharmacological treatments [3], [8], [10]–[12]. IPC devices work by inflated cuffs placed on the lower leg to apply compressions, thereby forcing the venous blood to move out of the leg. While IPC devices are effective at lowering the risk of DVT formation, is it still unknown what is the best timing profile for the devices with respect to the inflation rate of the cuffs, and the timing algorithm used to determine both when to trigger compressions and the frequency of compressions. By determining the effects of different timing profiles on the peripheral and central hemodynamics it could be possible to determine the most effective profile; this could improve the ability of the devices to prevent DVT.

1.2 Overview of the Circulatory System

The circulatory system is comprised of two subsystems, the pulmonary and systemic circulations, as shown in Fig. 1; this section herein will summarize from Silverthorn (2010) [20]. The pulmonary system sends deoxygenated blood from the right ventricle of the heart through the pulmonary arteries to the lungs, where the blood is oxygenated. The oxygenated blood returns through the pulmonary veins to the left atrium of the heart. In the systemic circulation, the more oxygenated blood is pumped from the left ventricle of the heart; the arteries then carry the oxygenated blood from the heart throughout the body. The veins work to return deoxygenated blood from the tissue to the heart. While the venous blood is not completely devoid of oxygen, it is carrying less than the arterial blood and is thus referred to as deoxygenated.

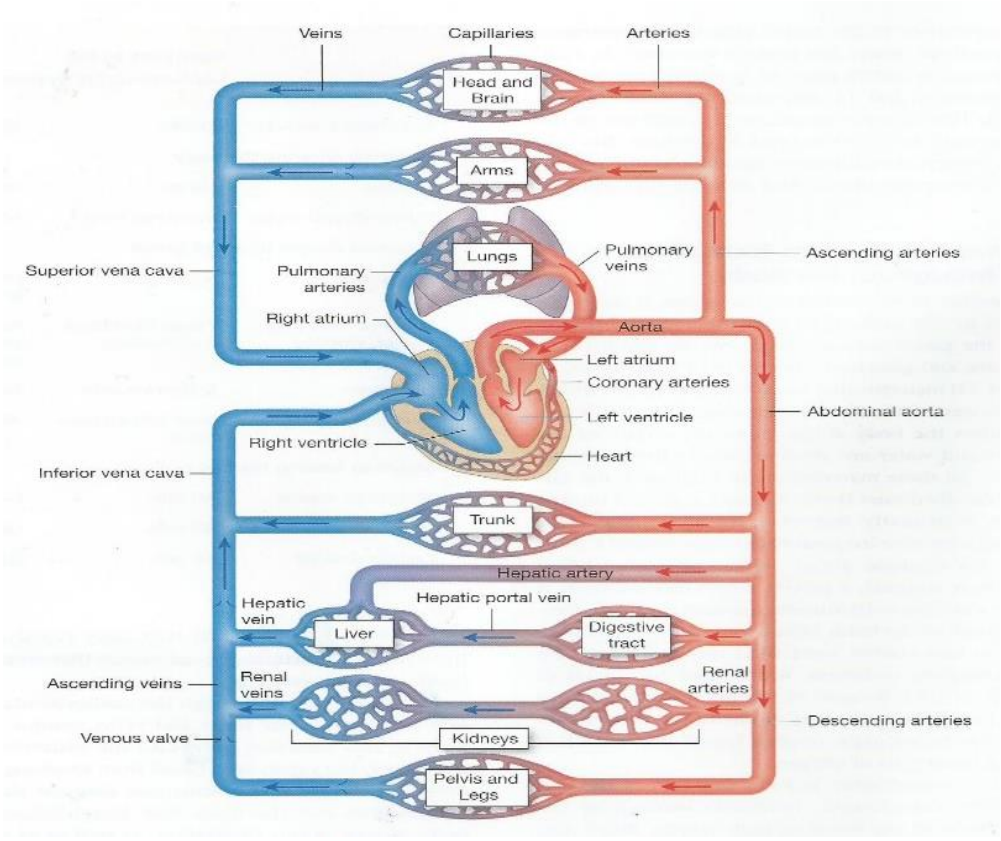

Fig. 1 Circulation of blood throughout the body through arteries and veins [20].

The flow of blood in the arteries is driven by the pressure wave from contraction of the left ventricle of the heart; due to the friction between the fluid and the vessel walls the pressure wave decreases over distance. This pressure wave disappears within the capillaries, as such the blood within the veins is not pulsatile. The veins are more compliant as they have thinner walls consisting of less elastic tissue than arteries, as such they are able to expand to accommodate venous pooling. The venous system serves as a volume reservoir for the body due to the larger diameter and more numerous quantity of veins in comparison to arteries.

A key contributor to the circulation of blood in the lower limbs is the muscle pump. The muscle pump functions as a “second heart” within the lower limbs, working to pump venous blood back to the heart. During ambulation, the muscles in the calf contract, applying force on the compliant veins and pushing the venous blood out of the limb, see Fig. 2. As the flow in the veins is not driven by the pressure of the cardiac cycle, they contain valves to prevent backflow.

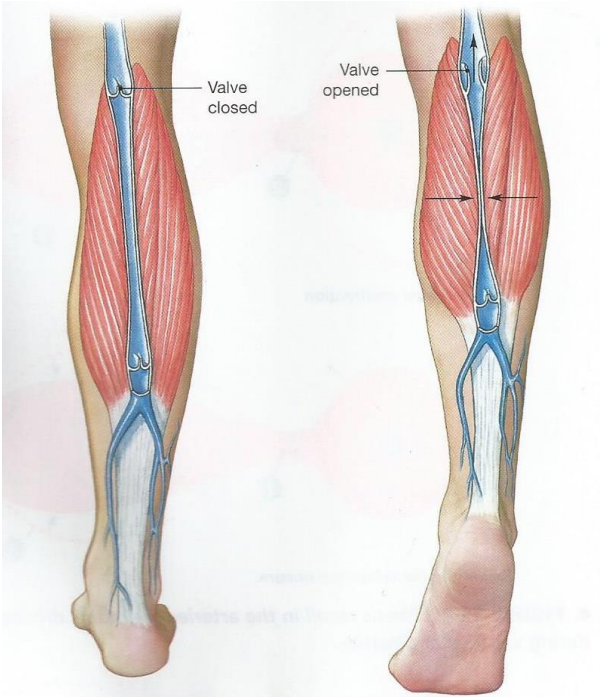

Fig. 2 Muscle pump's affect on veins [20].

The muscle pump has an effect on the pressure gradient within the circulatory system. The difference in pressure between the arteries and veins in the circulatory system is known as the arterial-venous pressure gradient; this difference is due to the high pressure that originates when arterial blood is pumped out of the heart and the decrease in pressure as the blood moves further from the heart, see Fig. 3. The muscle pump-induced venous return from the lower limbs increases this pressure gradient, and the arterial blood movement toward the lower pressure area in the limb, thereby improving the circulation [20], [21]. When a person is sedentary the muscle pump is not able to contribute to the venous return resulting in the venous blood pooling in the lower limb. This venous stasis in the legs is one of the factors that leads to DVT formation.

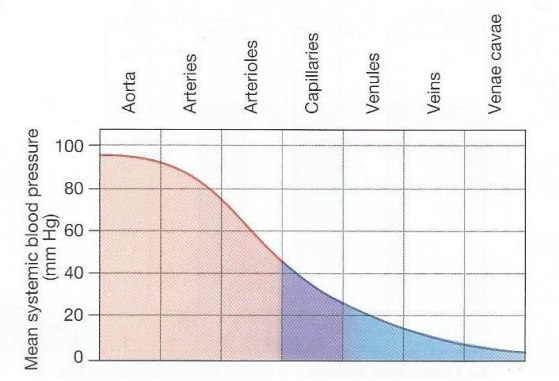

Fig. 3 Pressure gradient throughout the circulatory system [20].

1.3 Venous Thrombosis Initiation and Progression

Blood coagulation in the vascular system can be beneficial or dangerous depending on the circumstances surrounding the clot formation. The hemostatic system is responsible for clot formation [3], [20]. Clot formation is important when a vascular injury has occurred for the prevention of excessive bleeding and the clots dissolve after the injury has healed [3], [20]. However, the mechanisms for clot formation under normal circumstances are also involved in DVT creation in the absence of vessel injury. The composition of arterial and venous clots are different, with clots formed within veins primarily composed of fibrin, trapped red blood cells and platelets [3], [22], [23].

What causes the initiation of venous thrombosis is not fully known, however there are three primary factors that are known to influence DVT formation, namely hypercoagulability, vessel damage, and venous stasis [3]. Hypercoagulability is a condition where the blood is more prone to forming clots, this can be due to lower fibrinolytic activity [24]; fibrinolysis is the dissolution of fibrin by enzymes to remove clots [20]. Vessel damage can influence DVT if the body does not have a proper balance of the hemostatic response to an injury and results in blood clots forming on undamaged walls of the blood vessels [20]. Venous stasis can affect clot formation as it is hypothesized that the flow in the vessels has an effect on the formation and that reduced venous flow can be part of what triggers coagulation to stabilize the clot formation [3].

1.4 DVT Treatments

There are two key methods of DVT prophylaxis; anticoagulant drugs and mechanical compression to the lower limbs [3], [8], [11], [12]. Anticoagulant drugs are designed to treat the hypercoagulability factor and have been found to significantly lower the rate of DVT in clinical settings [14], [16]. Mechanical compression treats the venous stasis factor and can be applied through active or passive compression; both methods have been shown to lower the risk of DVT [14], [25]. Whereas passive compression is applied through the use of compression stockings, which work to mechanically limit the diameter of the deep veins thereby limiting the venous pooling that can occur [25], [26], active compression is applied through the use of devices capable of intermittently applying compressions to the lower limb. The active compression empties the pooled venous blood, which results in a change to the arterial-venous pressure gradient, thereby

increasing arterial inflow and overall peripheral circulation [21], [27]–[30]. Active compression systems have been shown to produce a similar effect to a muscle pump on the venous system in order to improve circulation in the lower limb [15], [16].

Both anticoagulants and mechanical compression methods have been proven to be effective, with combination treatments being the most effective [16], [25]. However, when used separately, anticoagulants and active compression have proven more effective than passive compression at DVT prevention [14], [25]. Drawbacks have been identified for each mitigation method that impact implementation and/or treatment outcome. A problem typically encountered with passive compression is poor fitting of the compression stockings, as this dramatically affects the pressure applied to the limb [25], [26]. A key challenge faced with prescribed active compression is the patient compliance; the duration and frequency of device use impacts the efficiency of DVT prevention [15]–[17], [25]. For example, patients that used an active compression device for more than six hours a day were at a significantly lower risk of forming venous blood clots than patients who used the device for less than six hours a day following their orthopaedic procedures [16]. Anticoagulants are associated with an increased risk of bleeding, which limits their prescription to particular patient populations [3], [8], [10]–[12]. Active compression has been identified as a preferred alternative treatment method to passive compression due to the increased effectiveness for DVT prevention and in cases where the bleeding complications eliminate anticoagulants treatment methods from consideration.

1.4.1 Active Mechanical Compression

Active mechanical compression is typically achieved through the use of IPC devices, see Fig. 4A, which have been proven to be an effective method of DVT prevention [6], [9]–[11], [15]–[18]. The cuffs of the device are placed on the lower limbs and inflated to apply compression to the limb, see Fig. 4B; thereby reducing venous stasis in the lower limb and preventing DVT formation [15], [31]–[33].

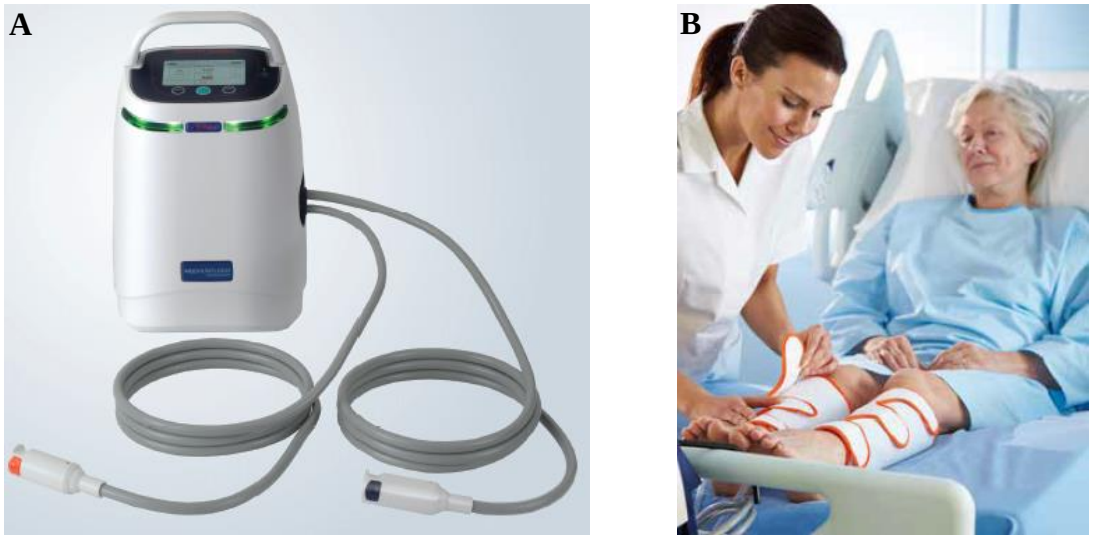

Fig. 4 Sample IPC device (A – Pump and tubing [34], B – Application of cuffs [35])

The inflation rate and duration of the compressions applied with the cuffs varies with each manufacturer but typically fall into two categories; rapid inflation with a short period of compressions or slow inflation and a longer period of compressions. It is still debated as to which device is more efficient at DVT prevention [6], [10], [15], [24]. Additionally, the frequency of compressions applied by the IPC devices also varies between devices, but is regulated by either fixed or "smart" timing algorithms. Fixed timing algorithms initiate compressions at set intervals that is not dictated by external signal measurements. "Smart" timing algorithms trigger compressions based on signal feedback from physiological measurements, which customizes the compression timing to an individual. Inflation rate and compression timing have been suggested to influence physiological response to treatment [9], [12], [18], [28], [36], [37].

1.4.2 Physiological Measurements

IPC device performance related to DVT prevention is typically assessed based on compression induced changes in peripheral venous hemodynamics [12], [15], [24], [36]–[38]. Specifically, the metrics of peak and average venous velocity during the compression period are used to quantify performance as these are taken to be representative of the device's ability to empty the venous blood from the lower limb and prevent venous stasis [12], [15], [24], [36]–[38]. Devices with compressions that consist of rapid inflation over short durations typically result in higher peak velocities while, devices which use profiles of slow inflation and have longer durations of compression typically will result in longer periods of increased venous velocity [6], [10], [15],

[24]. However, if is still debated whether peak velocity or average velocity is a better indication of DVT prevention [6], [10], [15], [24].

Morris *et al.* (2004) and Malone *et al.* (1999) noted that though there are flow differences that result from the inflation rate of the devices there has not been conclusive clinical proof as to whether a longer duration of increased velocity or a higher peak velocities is more effective at preventing DVT formation [6], [24]. Kakkos *et al.* (2005) and Warwick *et al.* (2008) similarly admit that it is unknown whether higher peak velocities or longer increases in velocity is the better mark of performance; however, both have different hypotheses as to which is the more effective measure [10], [15]. Kakkos *et al.* (2005) hypothesizes that the measure of longer periods of increased velocity is the better, as this might be an indication of reduced venous stasis in the valve pockets of the deep veins [10]. In contrast, Warwick *et al.* (2008) argue in favour of peak velocity, stating that it is a better indication of the IPC device's ability to mimic the turbulent, high velocity peripheral venous effects caused by ambulation [15]. However, it is also possible that there is a larger systemic response that cannot be fully studied by collecting only one measure of the peripheral hemodynamics.

1.4.3 "Smart" Timed IPC Devices

The majority of commercial devices use fixed timing, however there has been evidence that the use of "smart" timing algorithms may comparatively improve the performance of the IPC devices with respect to increased peripheral circulation [36]–[38]. For example, a device that times compressions based on the individual's venous refill rate has been shown to result in a longer duration of increased venous flow caused by compressions compared to similar devices that used slow inflation and longer periods of compression [36], [38], and a device that used a rapid inflation and shorter duration of compressions [36], [37].

The pulse-synchronized air-massage (PS-AM) device (Advance Co, Tokyo, Japan) triggers during the diastolic phase of the cardiac cycle, and has been proven to significantly increase the arterial blood flow in comparison to baseline measurements with no compressions applied [39]. Preliminary tests of the PS-AM device have also demonstrated significantly increased arterial blood flow when timed to the diastolic phase of the cardiac cycle, in comparison to fixed timing of the compressions at one second intervals [39].

A new cardiac gated compression (CGC) IPC device has been developed with a "smart" timing algorithm that utilizes prospective ECG gating technique and fixed pulse wave transit time from the heart to the lower limb compression location as inputs to determine when compression should be triggered. In addition, compression is initiated and completed during the local diastolic phase of the lower limb within a single cardiac cycle. The compression timing within the current cardiac cycle is based on the duration of the previous cardiac cycle, as such can vary from one cardiac cycle to the next depending on changes in heart rate. The CGC device has been shown to significantly increase both arterial and venous velocities during and after mild exercise [40].

The PS-AM device and the CGC device vary with respect to the method of detecting the cardiac cycle. The CGC device uses an ECG trace, whereas the PS-AM uses photoplethysmography (PPG) to detect the pulse from either the ear lobe or the fingers [39]. Furthermore, the CGC device completes a single compression cycle within one cardiac cycle, whereas the PS-AM requires four cardiac cycles to complete the compression cycle [39]. While the PS-AM device varies from the CGC device with respect to several design considerations, the results suggest that this form of "smart" timing will be efficient at increasing peripheral circulation.

1.5 Peripheral Sensor Considerations for "Smart" Compression Timing

Effectively timing a "smart" compression system requires real-time acquisition and processing of the controlling physiological signal. This can be heart rate or pulse arrival time in the case of cardiac-gated compression systems, or leg circumference in the case of venous refill time-based systems. The time-scale of the latter is much longer than that of the former, which requires much higher data rates and processing times. This section focuses on technologies that can be used for detecting the heartbeat, or local blood arrival time, for cardiac gated compression systems. Specifically discussed are sensors that use optical sensing, mechanical pressure, and bio-impedance. The choice of which sensor to use depends on the requirements of a given system. For cardiac gated compression systems, the primary concern is the reliability of pulse detection from the lower limb, compact size, and ease of use.

1.5.1 Photoplethysmography (PPG)

PPG is an optical technology that works by transmitting light into biological tissue and measuring the change in light intensity reflected back [41]. The light reflected back will contain an AC component to the signal which corresponds to the arterial blood volume changes and thereby the person's cardiac cycle [41]. The peaks of the PPG waveform have been proven to the correspond to the RR peaks of the ECG trace; proving that this method is capable of accurate pulse rate detection [41]–[43]. This method has also been shown previously to produce a measurable pulse signal from the lower limb and has been used as an monitoring tool for lower limb circulation [44]–[46]. Specifically, the pulse signal has been found from the calf [44], the anterior thigh region [45], and the anterior surface of the lower leg [46]. Based on the various regions on the leg that the PPG pulse sensor was able to detect the pulse it has been shown that this type of sensor does not require a location directly above a shallow artery in order to find the pulse signal. Furthermore, this method is commonly found in wearable HR monitoring technology due to its small profile and simplicity [47], [48]. However, key problems facing PPG technology are the sensitivity to both motion artifacts [41], [49] and skin pigmentations [50], [51].

1.5.2 Mechanical Pressure

The sensor that was based on mechanical pressure changes used a condenser microphone as the sensing component. A condenser microphone works as a pressure sensor to detect the pulse wave from the surface of the skin [52], [53]. The sensor can be small in size but have a high signal quality; as the diaphragm usually has a very small mass such that the sensor is largely immune to whole body movements [53]. The pulse signal detected by this type of sensor has been proven to correspond to an ECG trace when measured from the wrist [53]. Furthermore, measurements have been taken from the wrist, neck, forehead, inside and behind the ear [53]. However, these are all sites of relatively shallow arteries, it is unknown if this type of sensor could sense the pulse wave from deeper vessels of the lower limb. It is therefore possible that this sensor may be very sensitive to the measurement location making it harder to use across individuals.

1.5.3 Bio-impedance

Bio-impedance sensors work by placing pairs of emitter and receiver electrodes around an area of the body; the sensor will then emit an imperceptible electric current into the body and measuring

the change in impedance between the receiver electrodes [54]. This change in impedance if caused by fluid shifts; the sensor is able to detect the cyclic blood shifts caused by the cardiac cycle [54]. This method is typically used on the torso but has been shown to accurate detect the pulse signal from the forearm when compared to commercial pulse detection units [55]. This type of sensor is also very sensitive to motion artifacts [54], [55]. Furthermore, as multiple electrodes are required for the sensor to properly function this sensor will have a larger measurement area than the other two sensors considered. Finally, as the electrode placement can impact the signal quality [55], this sensor would require some training for individuals to use it properly.

1.6 Thesis Objectives

The focus of this thesis is on characterization and advancement of a novel cardiac gated compression system. This overall project is decomposed into two research directions, which this thesis attempts to advance: (1) comparing the system performance to existing commercial IPC devices, and (2) development of a new robust PPG sensor for detecting local pulse arrival for timing the compression system.

1.6.1 Study 1 Objectives

Component (1) is a comparative performance study between a custom cardiac-gated compression system developed in Mechanical and Mechatronics Engineering and Kinesiology at the University of Waterloo and existing commercial devices. More generally, this study aims to determine if IPC devices that use “smart” timing perform better than those with fixed timing and to test whether one form of “smart” timing is more efficient. To characterize the performance, the traditional metrics of peak venous velocity and average augmented velocity during the inflation period will be investigated. However, in order to have a better comparison of the effects of the IPC devices on systemic and peripheral hemodynamics; measurements of venous velocity, arterial velocity, stroke volume, heart rate, and muscle oxygenation were used to compare the performance of the devices.

1.6.2 Study 2 Objectives

For component (2), the primary objective is to develop a sensor and calibration cycle that would enable online determination of the optimal LED configuration and lowest possible intensity for an

individual's skin pigmentation and detection location. The primary focus is reliability and data fidelity, with a secondary consideration of optimizing battery life. Furthermore, the location on the lower limb that is most resistant to movement will be investigated to enable use of the sensor during rest and motion conditions.

1.7 Organization

This thesis is broken into three chapters. Chapter 2.0 covers the research that quantifies the performance of the CGC device in comparison to three other commercial IPC devices. Chapter 3.0 covers the results of the research into the performance of the pulse sensor designed for the periphery and its unique calibration cycle. Chapter 4.0 discusses the overarching results, limitations and conclusions of this thesis.

Chapter 2

2.1 Introduction

Intermittent pneumatic compression (IPC) is a proven mitigation strategy for deep vein thrombosis (DVT) formation in at-risk populations [11], [16]–[18]. Functionally, IPC emulates the muscle pump by mechanically compressing the veins, typically with inflatable air bladders, which squeezes the blood out of the venous system, thus reducing venous stasis and improving venous return to the heart [15], [31], [32], [56]. While similar in desired function, IPC devices vary with respect to key actuation parameters, including: the number and distribution of air bladders; the frequency and sequence of compressions (*e.g.*, uniform versus graded/sequential compression); inflation rate and duration; and the applied pressure levels.

Studies that aim to quantify the performance of IPC devices with respect to DVT prevention typically use only peripheral venous hemodynamic to comment on the performance of the device, with peak venous velocity and average flow during the compression period being the most common measures [12], [15], [24], [25], [37], [57]. Direct comparison studies between devices have found that multi-bladder systems that are sequentially inflated and/or have graded pressure from ankle to calf induce higher venous velocities than uniform pressure (typically single bladder) devices [31], [58], [59]. Inflation rate has also been shown to impact venous velocity, with rapid inflation devices eliciting higher peak venous flow rates, while slow inflation devices which inflate over a longer duration elicit longer periods of increased venous flow rates [9], [12], [15], [24], [37], [57]. From a clinical perspective, it is still a matter of some debate whether peak venous flow rate or duration of increased venous flow is a more important for mitigating DVT formation [6],

[10], [15], [24], though both measures indicate a reduction in venous stasis, which is directly correlated to clot formation.

Pressure and timing are both key factors in term of IPC performance. It has been shown that higher pressures result in greater emptying of the veins in the lower limbs [60]; however the timing of the compressions affects when this pressure is applied and how effectively it can be used. Though not common in commercial compression devices, there is evidence suggesting that timing algorithms based upon physiological measures of the user can further enhance peripheral circulation [10], [37], [57], [61]. The Kendall SCD Express estimates the venous refill time by actively measuring the calf circumference of the user during a calibration period and uses this measure to adjust the compression frequency [10], [37], [57], [61]. This "smart" timing algorithm has been shown to result in a longer duration of increased venous flow caused by compressions compared to similar devices that used slow inflation and longer periods of compression [38], [57], and a device that used a rapid inflation and shorter duration of compressions [37], [57]. Another form of "smart" timing uses photoplethysmography (PPG) to detect the pulse from either the ear lobe or the fingers and triggers compressions to begin during the diastolic phase of the heartbeat and completes a full compression cycle over four cardiac cycles [39]. This form of "smart" timing has been shown to significantly increased peripheral arterial blood flow when timed to the diastolic phase of the cardiac cycle, in comparison to fixed timing of the compressions at one second intervals [39].

Recently, we have developed and tested a rapid inflation/duration cardiac gated compression (CGC) device that times compressions to the heart beat detected via electrocardiography (ECG) and completes a full compression cycle within one heartbeat. We have demonstrated that this system significantly increases arterial inflow velocity and venous return velocity during and after mild exercise [40]. In this manuscript we aim to evaluate the performance of CGC versus other established timing modalities employed by commercial IPC systems. Specifically, we compare devices employing fixed versus "smart" timing, and slow versus rapid inflation rates to assess the impact of timing modality on peripheral and systemic circulation enhancement. We hypothesize that the systems employing "smart" timing will outperform the fixed frequency devices. We further hypothesize that the new CGC system will result in greater sustained circulation enhancement than the venous refill-based system.

2.2 Methods and Materials

2.2.1 Compression Systems

The study included four IPC devices with different compression timing profiles in order to compare the impact of this parameter on the central and peripheral hemodynamics. The key differences between the devices are the timing profiles and cuff segmentation. The characteristics of each device are summarized in Table 1. The ArjoHuntleigh Flowtron ACS800 (Flowtron) and the Kendall SCD Express (SCD) are both slow inflation devices while the Aircast VenaFlow Elite (VenaFlow) and cardiac gated compression (CGC) device are both rapid inflation devices. The Flowtron and the VenaFlow have a simpler, fixed frequency of compressions. Both the SCD and the CGC use different forms of "smart" timing to deliver compressions at a frequency that adapts to the individual. The SCD consistently applies pressure for 11 seconds however, the time between compressions varies between 20 to 60 seconds depending a calculated vein refill time [10]. The CGC device is a custom in-house developed system with a compression frequency dependent on the participant's heart rate and cuff inflation occurring during the local peripheral diastolic phase of each cardiac cycle.

Table 1: IPC Device Compression Profiles and Cuff Designs.

IPC Device	Cuff Design	Pressure (mmHg)	Compression Time (seconds)	Frequency of Compressions (compression/minute)	Inflation of Left/Right Cuffs
Cardiac Gated Compressions	Sequential, Circumferential (5 bladders)	50	0.3	Approx. 60 (based on heart rate)	Offset by half the total cycle time
ArjoHuntleigh Flowtron ACS800	Uniform, Asymmetric (1 bladder)	40	12	1 (fixed)	Offset by half the total cycle time
Kendall SCD Express	Sequential, Circumferential (3 bladders)	35 (proximal) 40 45 (distal)	11	0.8-1.9 (based on vascular refill time)	Offset by half the total cycle time
Aircast VenaFlow Elite	Sequential, Asymmetric (2 overlapping bladders)	45 (proximal) 52 (distal)	6 (distal bladder inflates in <0.5s)	1 (fixed)	Synchronous

A timing diagram is provided in Fig. 5 to help visualize the timing profile of each device. The duration of time the compressions for the left and right leg are applied in shown within a one-minute time span. It is assumed the left leg is the first to be compressed for the commercial devices. Furthermore, the compression period for the CGC device is too small to be easily noted however,

compressions to both the left and right legs occur between each of the vertical lines on the timeline. For plotting purposes, it is assumed the individual has a heartrate of 60 beats per minute (bpm) for the CGC device and has the minimum vascular refill time possible for the SCD.

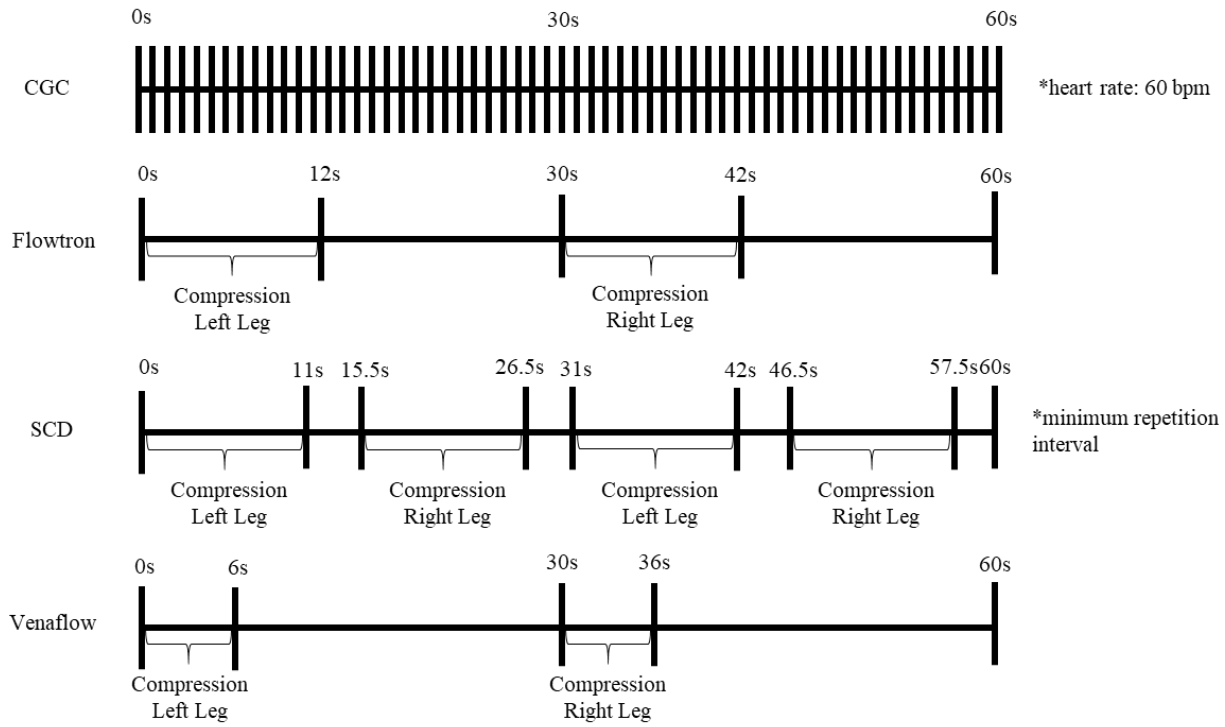

Fig. 5 Timing profiles showing compression duration and frequency for each IPC device in one minute

In order to remove the added variability of the effects of applied pressure, all devices were set to apply pressure within the range of 40-55 mmHg. Furthermore, all devices applied active compression to the lower limb with calf length cuffs.

2.2.2 Participants

The study participants included 12 healthy volunteers (6 males, 6 females) of age 26 ± 5.4 years with sedentary to moderate exercise lifestyles participated in the study. The average height and weights of the participants were 172.6 ± 8.3 cm and 70.0 ± 8.4 kg, respectively.

Individuals who had been diagnosed with or were currently being treated for cardiopulmonary conditions, skin sensitivities, or peripheral vascular sensitivity were excluded from participation in this study. Participants were asked to refrain from consuming alcohol, caffeinated beverages,

and from engaging in vigorous exercise during the 24-hour period prior to testing. Additionally, the participants were requested to refrain from consuming a large meal within the 2 hours of the testing period.

The experimental protocol for this study received clearance from the University of Waterloo Research Ethics Committee (ORE #21877) and conformed to the Declaration of Helsinki.

2.2.3 Experimental Protocol

The study was divided into two protocols, each occurring on separate days at approximately the same time of day. In each protocol, the participant was either seated in an upright position or supine with their legs slightly elevated. These postures were chosen to characterize the performance of the devices in positions typically occupied during prescribed use [16], [24]. The order of the protocols and the order in which the devices were tested were randomized between participants. For both body positions, the protocol was comprised of a one-minute baseline prior to the application of compression, a ten-minute compression period, and five-minute recovery period. All participants remained in the respective test body position for the duration of the protocol and asked to remain still to reduce data contamination from motion.

2.2.4 Data Collection

Data were collected continuously during the protocol with three time periods used to quantify the performance of the IPC devices; the baseline, the transient response, and the steady state response to compressions. The baseline prior to the start of compressions is used as a reference period to assess the transient and steady state response to compression. The transient response was evaluated based on the average of the first minute of compressions, spanning the first compression of the fixed timing devices and the first several compressions of the “smart” timing IPC devices depending on the individual’s heart rate and vascular refill time. The steady state condition achieved with the application of compression devices was taken as the average response over the three last compression periods for the metrics of peak venous velocity and average venous displacement during compression. The steady state condition for all other measures was taken as the average response over the last minute of compression.

A standard 3-lead chest electrocardiogram (ECG; Pilot 9200, Colin Medical Instruments, San Antonio, TX) was used for heart rate (HR) measurements, which were recorded at a sampling frequency of 1kHz. A photoplethysmography cuff (Finometer, Finapres Medical Systems, Amsterdam, Netherlands) was placed on the middle finger of the right hand to continuously monitor the local arterial pressure wave. The cardiac stroke volume (SV) of the participant was determined from the analysis of the pressure wave using the Modelflow ® algorithm (Finapres Medical Systems, Amsterdam, Netherlands). Data were collected at a sampling frequency of 1 kHz.

A 4-MHz Doppler ultrasound probe (WAKI^{e}, Atys medical, France) was used to continuously record the venous velocity from the femoral vein in the right leg. Venous velocity data were collected at a sampling frequency of 200 Hz. The peak venous velocity and the average volume of venous blood ejected during the last three compression cycles were used to quantify the IPC devices' performance which is on par with published metrics for IPC systems [9], [10], [12], [15], [24], [37], [57]. The average volume measures are used to estimate the total venous displacement resulting from compression over an hour [10], [37], [57]. These metrics were calculated with the volume measures being replaced with displacement to account for the lack of venous diameters. This study also examined the average venous velocity over the first and last minute to determine the average velocity in the limb beyond just the compression period. HR, SV, and venous velocity measurements were concurrently acquired using a Powerlab data acquisition system (Powerlab, ADInstruments, Colorado Springs, Colorado, USA).

Echo Doppler ultrasound (Mindray M5, Shenzen Mindray Bio-medical Electronics, Shenzen, China) was used to record the arterial velocity from the superficial femoral artery (SFA) in the left leg at the set three time points of interest during the testing. Arterial velocity data were collected at a sampling frequency of 125 Hz. A Near-Infrared Spectroscopy (NIRS) probe (PortaLite, Artinis Medical Systems B.V., Elst, The Netherlands) was placed on the back of the left calf over the lateral head of the gastrocnemius muscle to continuously measure the muscle oxygenation. The NIRS data were separated into measures of the concentrations of the oxygenated hemoglobin (O_2Hb), deoxygenated hemoglobin (HHb), and total hemoglobin (tHb), which were collected at three depths; however, only the measures at the deepest penetration depth were analyzed to compare the changes in hemoglobin concentrations caused by compressions. All NIRS

measurements were collected at a sampling frequency of 50 Hz. NIRS measurements were collected on eleven of the twelve study participants.

2.2.5 Statistical Analysis

Both the supine and seated data underwent the same statistical analysis. For each of the physiological measurements, mixed effects models were used to model the measurement response based on the fixed effects of time and device, and the random effect of the participants. The quantile-quantile (QQ) plots of the data sets for this study showed that the models were good fits for the data. However, there was minor divergence from the tails of the QQ plots for the arterial velocity, the O_2Hb concentration and the venous peak velocity data sets from the seated protocol.

The initial level of significance used for the statistical analysis was an alpha value of 0.05. The Bonferroni method was used to adjust the level of significance to protect against multiple comparison errors [62]. Hypothesis tests were conducted with pairwise t-tests.

The device factor used six pairs of comparisons to compare each of the four devices to one another. The peak velocity and displacement measurements had a simplified time factor, as such the Bonferroni adjusted level of significance of the data becomes $p<0.008$. For all other measures the time factor used two paired comparisons to compare each of the time points during compression (first minute of compressions, and last minute of compressions) to the baseline values. Due to an interaction effect between the fixed factors the Bonferroni adjusted level of significance of the data becomes $p<0.004$.

2.3 Results

2.3.1 Central Hemodynamics

Table 2 and **Error! Reference source not found.** presents pooled heart rate (HR), stroke volume (SV), and cardiac output (CO) data for all devices during baseline, the first minute of compressions, considered the transient state, and the last minute of compression, considered the steady state configuration, for the seated and supine protocols respectively. CGC showed significantly increased SV maintained throughout the compression period, as well as a slight decrease in HR during steady state. There was a trend towards increased SV in steady state for the

Flowtron device. However, all three commercial devices demonstrated significantly lower SV than the CGC device for the duration of compression. Furthermore, CO was increased during the transient stage for the CGC device only; adaptation occurred by the steady state time point such the SV increase was compensated by a HR decrease, resulting in only a trend towards increased CO (p=0.1). The SCD and Flowtron devices exhibited lower CO than the CGC device during the transient phase, while the VenaFlow and the SCD were lower and significantly lower, respectively, from the CGC in the steady state.

Table 2: Central hemodynamic results throughout the seated compression protocol. Results are shown (mean ± std) for all compression devices at the baseline (1 minute before the start of compressions), the transient state (first minute of compressions), and the steady state (last minute of compressions). Significant interaction effects are denoted as follows: *Results are different (p<0.05) from baseline; **Results are significantly different (p<0.004) from baseline; #Results are different (p<0.05) from CGC at the corresponding time point; ##Results are significantly different (p<0.004) from CGC at the corresponding time point.

	Baseline	First Minute	Last Minute
Heart Rate (bpm)			
CGC	67.9 ± 10.6	66.8 ± 9.5	65.3 ± 9.4 *
Flowtron	69.6 ± 11.9	69.1 ± 10.7	68.3 ± 9.6 #
SCD	69.5 ± 12.5	68.9 ± 11.0	67.3 ± 9.8
VenaFlow	68.4 ± 10.9	66.6 ± 9.4	66.7 ± 8.6
Stroke Volume (mL)			
CGC	81.3 ± 19.8	88.1 ± 19.5 **	87.7 ± 19.3 **
Flowtron	75.9 ± 21.9	77.3 ± 20.1 ##	79.2 ± 22.8 * ##
SCD	76.5 ± 23.1	78.0 ± 22.2 ##	76.2 ± 22.2 ##
VenaFlow	78.2 ± 16.6	81.1 ± 17.2 ##	79.3 ± 20.8 ##
Cardiac Output (L/min)			
CGC	5.4 ± 0.9	5.8 ± 1.1 *	5.7 ± 1.0
Flowtron	5.2 ± 1.3	5.3 ± 1.3 #	5.4 ± 1.5
SCD	5.2 ± 1.5	5.3 ± 1.3 #	5.1 ± 1.3 ##
VenaFlow	5.3 ± 1.3	5.4 ± 1.3	5.2 ± 1.3 #

Table 3: Central hemodynamic results throughout the supine compression protocol. Results are shown (mean ± std) for all compression devices at the baseline (1 minute before the start of compressions), the transient state (first minute of compressions), and the steady state (last minute of compressions). Significant interaction effects are denoted as follows: *Results are different (p<0.05) from baseline; #Results are different (p<0.05) from CGC at the corresponding time point; +Results are different (p<0.05) from VenaFlow; ++Results are significantly different (p<0.004) from VenaFlow.

	Baseline	First Minute	Last Minute
Heart Rate (bpm)			
CGC	61.3 ± 9.0	62.5 ± 10.1	62.2 ± 9.8
Flowtron	62.5 ± 9.5	61.0 ± 10.0	63.9 ± 10.4 +
SCD	62.7 ± 11.5	60.3 ± 10.1 * #	63.3 ± 11.1
VenaFlow	62.4 ± 8.5	60.8 ± 9.3	61.3 ± 9.1
Stroke Volume (mL)			
CGC	84.5 ± 17.6	85.8 ± 19.0	84.0 ± 19.4
Flowtron	83.4 ± 12.7	85.1 ± 13.9	86.1 ± 16.3
SCD	84.5 ± 15.4	86.3 ± 15.8	85.3 ± 18.5
VenaFlow	81.2 ± 18.3	82.8 ± 17.5	81.5 ± 17.4

Cardiac Output (L/min)			
CGC	5.1 ± 1.1	5.3 ± 1.2	5.2 ± 1.2
Flowtron	5.2 ± 1.2	5.2 ± 1.2	5.5 ± 1.2 ++
SCD	5.3 ± 1.3	5.1 ± 1.1	5.3 ± 1.3 +
VenaFlow	5.0 ± 1.2	5.0 ± 1.1	5.0 ± 1.2

The CO results for the SCD and Flowtron devices were lower and significantly lower, respectively, from the VenaFlow device during the steady state. Otherwise there is a minor decrease in HR produced by the SCD during the first minute but the change is not maintained. Finally, there is a decrease in the HR in the last minute for the Flowtron. In general, the differences between the devices are more significant when seated, thus highlighting the dependence of IPC device performance on position [61].

2.3.2 Arterial Velocity

The superficial femoral arterial velocity for both the seated and supine protocols is presented in Fig. 6. In the supine position (Fig. 6A), increased velocity relative to baseline was maintained by the CGC device throughout duration of compressions. The Flowtron exhibited elevated flow during steady state. Flowtron and SCD produced lower and significantly lower femoral velocities compared with CGC in the first minute of compressions, respectively, whereas the VenaFlow was the only device producing statistically lower velocities than CGC in steady state.

More pronounced effects of CGC were found during the seated protocol (Fig. 6B). In this position, CGC was the only device that resulted in significantly elevated arterial velocities from baseline for the duration of compressions; the Flowtron showed significantly elevated arterial velocities during the first minute only. All commercial devices produced lower arterial velocities than CGC throughout compression. Both SCD and VenaFlow were lower than Flowtron as well during the first minute of compressions.

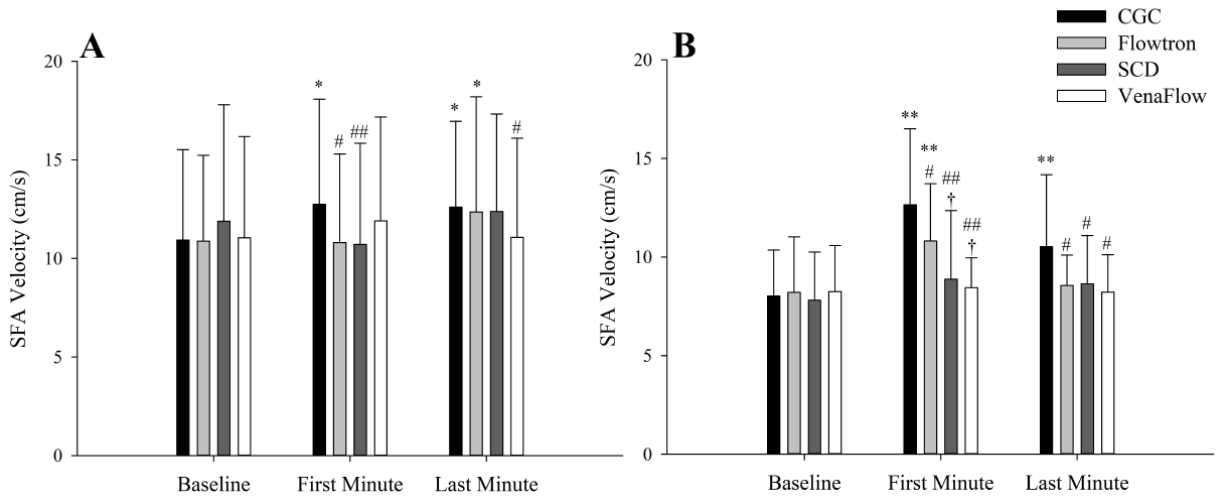

Fig. 6 Arterial beat-by-beat velocity in the superficial femoral artery of the left leg (A – Supine, B – Seated). Results are shown (mean ± std) for all compression devices at the baseline (1 minute before the start of compressions), the transient state (first minute of compressions), and the steady state (last minute of compressions). Significant interaction effects are denoted as follows: *Results are different ($p<0.05$) from baseline; **Results are significantly different ($p<0.004$) from baseline; #Results are different ($p<0.05$) from CGC at the corresponding time point; ##Results are significantly different ($p<0.004$) from CGC at the corresponding time point; †Results are different ($p<0.05$) from Flowtron at the corresponding time point.

2.3.3 Venous Velocity

Average femoral venous velocities over one minute intervals are presented in Fig. 7 for both body positions. Within the supine prosition the Flowtron and SCD baseline velocities were increased in comparison to the Flowtron baseline velocity; however, as none of these devices resulted in siginficant changes from their baseline values in this position it is unlike this initial difference affected the statistical results for the comparisons between the devices at later time points. In comparison with baseline, the CGC device resulted in significantly increased velocities during the first minute of compressions in both body positions; the Flowtron showed an increase during the first minute in the seated protocol. Comparing compression devices, CGC showed significantly greater velocities than the other devices during the first minute of compression while seated, and increased and significantly increased velocity compared to the SCD and VenaFlow, respectively, during the first minute while supine. In the last minute of compressions, none of the devices showed increased velocity with respect to baseline. All devices were similar in the last minute, with the exception of the VenaFlow while seated, which had lower velocity that CGC.

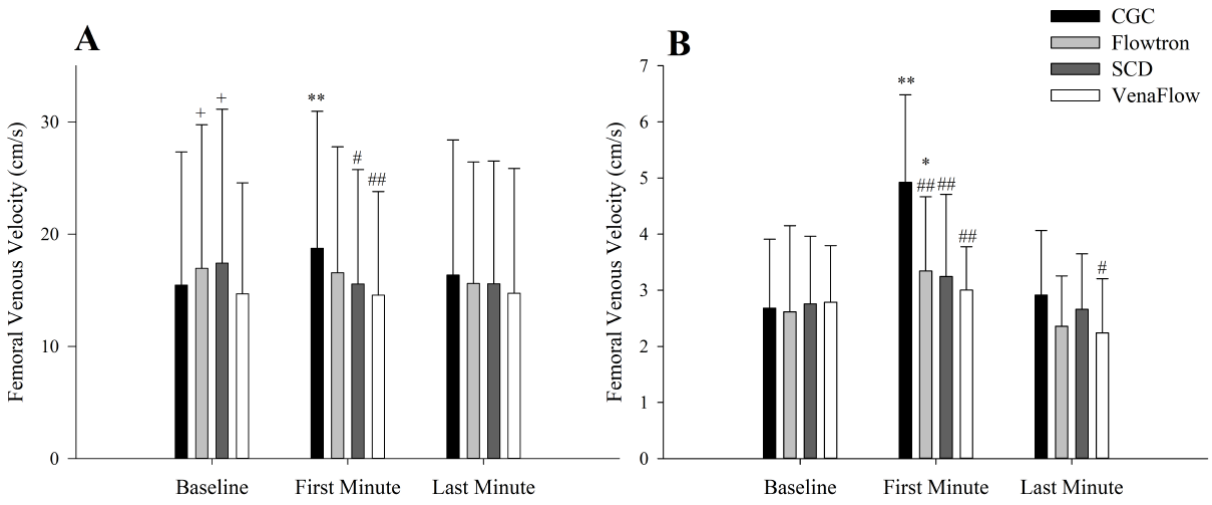

Fig. 7 Venous velocity averaged over one-minute time points in the femoral vein of the right leg (A – Supine, B – Seated). Results are shown (mean ± std) for all compression devices at the baseline (1 minute before the start of compressions), the transient state (first minute of compressions), and the steady state (last minute of compressions). Significant interaction effects are denoted as follows: *Results are different ($p<0.05$) from baseline; **Results are significantly different ($p<0.004$) from baseline; #Results are different ($p<0.05$) from CGC at the corresponding time point; ##Results are significantly different ($p<0.004$) from CGC at the corresponding time point; +Results are different ($p<0.05$) from VenaFlow at the corresponding time point.

The average velocities presented in Fig. 7 include both the periods when compression is applied, as well as the time between compressions. Several prior studies, in contrast, have assessed IPC performance by considering instead the maximum venous velocity observed during steady state compressions only during the time in which compression is applied [9], [15], [24], [37], [57]. To facilitate direct comparison with these studies, Fig. 8 presents the average peak velocity of the last 3 compressions in each protocol for all devices considered. In the supine position (Fig. 8A), all devices except CGC show significantly higher peak velocity compared with baseline and CGC, with VenaFlow being significantly higher than all other devices. In the seated posture (Fig. 8B), all devices produced significantly elevated peak velocities compared with baseline. As with the supine, VenaFlow had significantly higher peak velocity than the other devices, whereas Flowtron was significantly higher than CGC.

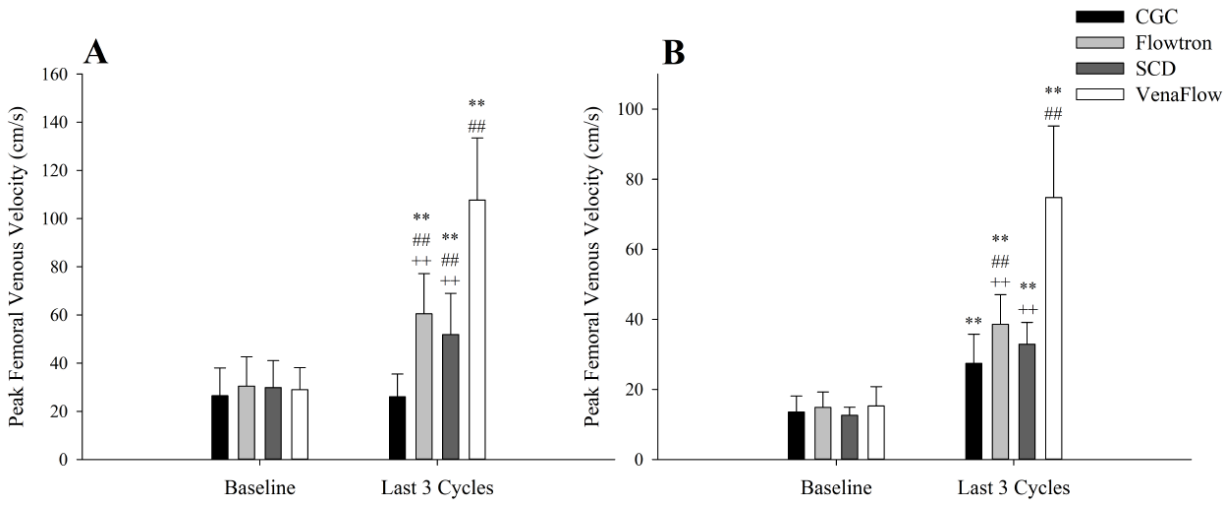

Fig. 8 Peak venous velocity in the femoral vein of the right leg averaged over 3 cycles within the steady state condition (A – Supine, B – Seated). Results are shown (mean ± std) for all compression devices at the steady state time point (last 3 compression cycles). Significant interaction effects are denoted as follows: **Results are significantly different ($p<0.008$) from baseline; ##Results are significantly different ($p<0.008$) from CGC; ++Results are significantly different ($p<0.008$) from VenaFlow.

2.3.4 Venous Displacement

In an effort to enable meaningful comparisons between devices with disparate compression durations and frequencies, the venous displacements are calculated for one compression period, the results of which are presented in Table 4. Also included is an estimate of the venous displacement that would be achieved after an hour of steady state compressions. All commercial devices had significantly larger displacements per compression than CGC, with Flowtron and SCD also displacing the blood further than the VenaFlow in both positions. Over the course of an hour, however, CGC in the seated position produces significantly larger displacements than the other devices due to the much higher compression frequency. Similarly, the SCD outperforms the Flowtron in the seated position, possibly due to the compression frequency. In the supine position, Flowtron and SCD outperform the VenaFlow; the SCD also outperforms the CGC. Subject to subject variability, as evidenced by the standard deviation of the results, was generally much larger in the supine position.

Table 4: Venous displacement in the femoral vein throughout the seated and supine protocols. Results are shown (mean ± std) for all compression devices at the steady state time point (last 3 compression cycles). Significant interaction effects are denoted as follows: ##Results are significantly different ($p<0.008$) from CGC; +Results are different ($p<0.05$) from VenaFlow; ++Results are significantly different ($p<0.008$) from VenaFlow; ††Results are significantly different ($p<0.008$) from Flowtron.

	Supine	Seated
Mean Displacement per compression (cm)		
CGC	3.4 ± 1.8	2.3 ± 0.8
Flowtron	272.2 ± 144.0 ## ++	95.8 ± 27.5 ## ++
SCD	243.1 ± 131.3 ## +	97.2 ± 27.9 ## ++
VenaFlow	180.3 ± 81.9 ##	75.8 ± 17.5 ##
Mean Displacement per hr (cm)		
CGC	13303.5 ± 8637.8	8826.2 ± 2935.2
Flowtron	16332.7 ± 8640.1 ++	5749.9 ± 1651.0 ## +
SCD	18289.5 ± 8456.3 ## ++	7270.5 ± 2037.4 ## ++ ††
VenaFlow	10815.1 ± 4911.3	4545.0 ± 1052.1 ##

2.3.5 Muscle Oxygenation

Tables 5 and 6 present the muscle oxygenation data for the supine and seated protocols, respectively. For both positions, all devices induced significantly lower HHb and tHb concentrations during steady state operation in comparison with baseline values, thus demonstrating the ability of all devices to remove the venous pooling in the lower limbs. Only CGC resulted in a sustained effect on the O_2Hb concentration as well. Comparing devices, CGC was significantly different from the commercial systems in all measures except for O_2Hb concentration in the supine position for the Flowtron device. We note that the baseline value for Flowtron, however, was significantly different from CGC; the change in O_2Hb concentration from baseline was, in fact, significantly different than CGC during the first minute ($p=1.53 \times 10^{-5}$) and last minute ($p=1.32 \times 10^{-6}$), in alignment with all other devices.

Table 5: Muscle oxygenation values throughout the supine compression protocol. Results are shown (mean ± std) for all compression devices at the baseline (1 minute before the start of compressions), the transient state (first minute of compressions), and the steady state (last minute of compressions). Significant interaction effects are denoted as follows: *Results are different ($p<0.05$) from baseline; **Results are significantly different ($p<0.004$) from baseline; ##Results are significantly different ($p<0.004$) from CGC at the corresponding time point; †Results are different ($p<0.05$) from Flowtron at the corresponding time point; ††Results are significantly ($p<0.004$) different from Flowtron at the corresponding time point; &Results are different ($p<0.05$) from SCD in the corresponding protocol.

	Baseline	First Minute	Last Minute
O_2Hb (Δμm)			
CGC	1.0 ± 2.4	-2.4 ± 2.0 **	-1.7 ± 2.3 **
Flowtron	-0.5 ± 1.6 ##	-1.6 ± 1.9 *	-0.8 ± 2.0
SCD	0.5 ± 1.4 †	-0.2 ± 2.0 ## ††	0.0 ± 2.3 ##
VenaFlow	0.9 ± 2.1 ††	0.0 ± 1.9 ## ††	0.0 ± 2.6 ##

HHb (Δμm)			
CGC	-2.3 ± 2.5	-5.0 ± 2.6 **	-6.1 ± 2.8 **
Flowtron	-1.9 ± 3.1	-3.0 ± 3.2 * ##	-4.0 ± 3.6 ** ##
SCD	-1.8 ± 3.2	-3.2 ± 3.4 ** ##	-4.2 ± 3.6 ** ##
VenaFlow	-1.8 ± 2.7	-2.5 ± 2.6 ##	-3.4 ± 3.1 ** ## &
tHb (Δμm)			
CGC	-1.3 ± 3.9	-7.4 ± 3.2 **	-7.7 ± 3.3 **
Flowtron	-2.3 ± 3.7	-4.6 ± 4.1 ** ##	-4.8 ± 4.2 ** ##
SCD	-1.3 ± 4.0	-3.4 ± 4.3 ** ##	-4.2 ± 4.5 ** ##
VenaFlow	-1.0 ± 4.0 †	-2.4 ± 3.4 * ## ††	-3.3 ± 4.2 ** ## †

Table 6: Muscle oxygenation values throughout the seated compression protocol. Results are shown (mean ± std) for all compression devices at the baseline (1 minute before the start of compressions), the transient state (first minute of compressions), and the steady state (last minute of compressions). Significant interaction effects are denoted as follows: *Results are different ($p<0.05$) from baseline; **Results are significantly different ($p<0.004$) from baseline; ##Results are significantly different ($p<0.004$) from CGC at the corresponding time point.

	Baseline	First Minute	Last Minute
O_2Hb (Δμm)			
CGC	2.4 ± 2.7	-3.2 ± 4.5 **	-1.7 ± 4.8 **
Flowtron	2.3 ± 2.2	1.0 ± 2.5 ##	0.8 ± 2.6 * ##
SCD	1.8 ± 1.9	1.2 ± 1.8 ##	0.7 ± 2.4 ##
VenaFlow	2.9 ± 3.5	1.7 ± 3.6 ##	1.0 ± 3.1 * ##
HHb (Δμm)			
CGC	-2.3 ± 2.6	-6.9 ± 2.1 **	-8.5 ± 2.3 **
Flowtron	-1.1 ± 2.8	-2.5 ± 2.8 * ##	-4.5 ± 3.2 ** ##
SCD	-1.3 ± 2.3	-3.4 ± 2.1 ** ##	-4.8 ± 2.6 ** ##
VenaFlow	-1.3 ± 2.5	-2.1 ± 2.1 ##	-4.7 ± 2.3 ** ##
tHb (Δμm)			
CGC	0.0 ± 4.0	-10.1 ± 5.1 **	-10.2 ± 6.0 **
Flowtron	1.2 ± 2.6	-1.5 ± 2.9 * ##	-3.8 ± 3.9 ** ##
SCD	0.5 ± 3.0	-2.1 ± 2.6 * ##	-4.1 ± 3.5 ** ##
VenaFlow	1.6 ± 3.9	-0.5 ± 3.7 ##	-3.7 ± 3.7 ** ##

During the first minute of compression, SCD and the CGC exhibited significantly lower HHb concentrations and Flowtron showed modest change. All devices reduced tHb in the first minute of compressions with the exception of the VenaFlow while seated. Only CGC significantly impacted O_2Hb concentration in the first minute of compression. In general, device performance was similar for the two postures, suggesting an insensitivity of muscle oxygenation to body position.

2.4 Discussion

2.4.1 Hemodynamic Comparison of the Timing of the Devices

The CGC system, with its rapid inflation and high frequency, was the only device to produce a sustained increase in SV for the duration of the compression in either posture. A similar effect was found by Bickel *et al*. (2011), in which they observed a maintained increase in SV when compression was applied twice per minute; however they also saw an increase in the CO [63]. Despite elevated SV for CGC, slight reductions in HR result in CO being only slightly elevated ($p=0.1$). Though considerably lower in frequency than CGC, two compressions per minute is still generally a higher rate of compression than the three commercial devices tested in this study (SCD can have similar compression frequency, depending on venous refill time, see Table 1). As such the increased SV could be due to the frequency of compressions and the difference in CO results may be due to differences in the subject population (all men vs men and woman in this study), the cuff length (foot to thigh vs calf), or the measurement posture (left lateral decubitus position vs seated/supine) as the positional differences have been shown to affect results in this study and others [61]. Bickel *et al*. (2011) attributed the increase in CO to the decrease in total peripheral resistance (TPR) and an increased venous return [63]. Due to the insignificant change to the CO for the CGC the increase is SV is not likely due to a significant change in TPR as the CO and TPR are inversely related. Instead the change in SV by the CGC may be due to the compressions causing an increase in the arterial-venous pressure gradient; as upon the release of compression, blood flow into the limb has been shown briefly elevate due to a transient increase in the arterial-venous pressure gradient [25], [27], [64]–[66]. This would result in a higher preload and also explains the greater effect in the seated position, as the pressure difference is greater than in supine as the legs are further from heart level.

The increase in arterial-venous pressure, flow enhancement mechanism should be common to all devices. However, CGC and Flowtron were the only devices to increase the SV at steady state in the seated position. Furthermore, they were the only devices to increase SFA velocity and the average femoral venous velocity, with CGC being the only one to sustain the increase on the SFA beyond the first minute of compressions. Additionally, the CGC showed significantly greater venous velocities than the other devices during the transient state while seated; this result suggests

that the CGC device may be more efficient at eliminating the venous pooling that results from the seated position. Interestingly, these two devices are on opposite ends of the complexity spectrum, as shown in Table 1. The transient effects of the Flowtron are potentially demonstrating the slower devices abilities to quickly eliminate the increased venous pooling due to the seated position, the slower device may perform better than the VenaFlow as the duration of compression is longer causing a greater displacement of venous blood. However, as the effect on the arterial velocity is not maintained this could suggest that the CGC's compressions are more efficient at improving peripheral circulation. The frequency of the CGC's compressions could have a greater effect on the arterial-venous pressure gradient as the increase in venous velocity during the transient phase is significantly greater than the other devices. The frequency of compression timing could work to maintain the lower venous pressure which accounts for the consistently increased inflow of the arterial blood to the lower limb. We note that during the first minute of compressions, the SCD has already gone through it's calibration cycle comparing it to other devices at the start of compressions is not strictly prudent as it does not have the same venous pooling to act upon. It performs no better than any of the commercial devices in the steady state, however, at which point ample time had elapsed for all devices to reach the same steady state behaviour.

IPC devices with rapid inflation profiles have been shown to produce significantly higher peak venous velocities in comparison with slower inflating devices [9], [15], [24], [37], [57]. In alignment with these findings, this study finds that the VenaFlow resulted in significant higher peak venous velocity compared to the SCD and Flowtron units. The low frequency, rapid inflation compression profile of the VenaFlow rapidly ejects the blood from the veins, resulting in high peak venous velocities. The CGC device, despite having the most rapid inflation rate of the compared devices, had the lowest peak venous velocities of all devices due to the very high frequency of compression, which allowed little venous refilling between subsequent actuation events. The SCD, which could have higher compression frequencies than the Flowtron and Venaflow, had the next lowest peak venous velocity, further suggesting that frequency, and not just inflation rate, is an important performance parameter. While the peak venous velocity at steady state was elevated from baseline for most cases, the velocity minute averages at steady state showed that none of the devices elicited values significantly different from baseline. This suggests that potentially the devices are all capable of eliminating venous stasis, but the periods of augmented venous flow are confined to the compression periods once at steady state.

IPC devices with slower inflation and longer duration compression profiles have been shown to result in prolonged increases in velocity during the compression period [9], [10], [37], [57]. As such, the average volume of venous blood ejected per compression and over an hour period of compressions, has been shown to be higher for slow inflation devices in comparison to rapid inflation [9], [37], [57]. In this study, it was found that the slow inflation devices (Flowtron and SCD) did outperform the rapid inflation devices (VenaFlow and CGC) in the venous displacement per compression. Flowtron and SCD resulted in the greatest (though equivalent) displacement per compression likely due to their slower inflation cycles having longer periods of venous velocity augmentation. The VenaFlow did result in significantly greater displacement per compression than the CGC, again due to the vast disparity in actuation frequency and the resultant impact on venous refilling between compressions.

Though exhibiting the smallest venous displacement per compression, over the course of a simulated one-hour compression therapy session, CGC outperformed all other devices in the seated protocol and was similar to the other devices for the supine position. This suggests that rapid, high frequency inflation, can perform at least as well as the slow, long duration compression protocols; assuming that there is not a significantly different impact on diameter by the devices as this metric was not measured but could impact the comparative behaviour. The SCD and Flowtron had greater displacements per hour than the VenaFlow in both postures, in alignment with the prior compression results. Interestingly, despite employing "smart" timing, the SCD did not outperform the simpler Flowtron device in any venous blood movement measure (peak velocity, average velocity, or blood displacement). These results contrast with Griffin *et al*. (2007), whose study found superior performance of the SCD over a similar Flowtron model [57]. However, this may be due in part to differences in cuff length (thigh length cuffs versus calf length in this study), test posture (semi-recumbent versus seated/supine), or the subject population (varicose veins versus no venous insufficiencies) [57].

The muscle oxygenation results matched the trends seen in the arterial velocity and SV measures. The two "smart" timing devices, CGC and SCD, both resulted in a sustained decrease in de-oxygenated hemoglobin throughout the duration of the study. The CGC also resulted in significantly lower concentrations of tHb in comparison to the other devices at both the transient and steady state in both postures, suggesting that the "smart" timing used by the CGC device is

more beneficial and faster to take effect than the devices which use fixed timing. Finally, only the CGC resulted in a sustained effect on the oxygenated hemoglobin concentration during the transient and steady state conditions in both positions, further indicative of the sustained ability of the device to improve the peripheral circulation, as also found with SFA velocity and SV data.

2.4.2 Quantitative Measures to Determine Performance

The manufacturers of the majority of commercially available IPC devices relate performance of the device to the venous measures collected during the portion of the cycle when the device is applying pressure [15]. The means of quantifying the venous return resulting from application of the devices vary. It is a matter of some debate whether it is better to have a higher maximum venous velocity or a sustained increase in average venous velocity during the compression period [6], [10], [15], [24].

It is possible that the venous measurements are not the best measure of IPC performance. Lurie *et al.* (2008) reported results contrary to the common assumption that the hemodynamic response to IPC devices can be attributed solely to the deep veins, instead observing that the superficial veins and potential fluid shifts into the intravascular space may play a significant role [67]. Another possible flaw in the peak venous velocity and venous displacement measures is that they do not take into account the velocity of the venous blood during the time in which the cuffs are not inflated. Furthermore, the measurements are usually only taken from one vein. As such it is not possible to visualize the full picture of what is truly occurring with the venous return. However even the minute averages of the venous velocity were not indicative of performance when compared to the other physiological measurements.

The measures of the stroke volume, arterial velocity and muscle oxygenation all showed fairly consistent results for the performance of the devices at each time point. Based on the similarities in results outside of the venous measurements it may be better in the future to use arterial velocities instead of venous to quantify the performance of IPC devices. Additionally, having multiple measures to examine the effect of the IPC devices is likely to help quantify the effect of the IPC device on not just the peripheral but the systemic hemodynamics.

2.5 Conclusions

The CGC device outperforms the commercial devices in the seated position, while performing at least as well as the other devices in the supine position, for virtually all objective performance measures, except for peak venous velocity and venous displacement per compression. The VenaFlow outperformed all devices with respect to higher peak venous velocities. The Flowtron and SCD had the greatest venous displacements per compression. Both the CGC and the VenaFlow are rapid inflation devices with sequentially inflated cuffs. The CGC outperformed the VenaFlow in the majority of the hemodynamic responses measures when seated, suggesting that the complexity of the "smart" timing likely in combination with the higher frequency of inflation resulted in improved performance. While the SCD and Flowtron are both slow inflation devices, in this case the "smart" timing used to time the SCD's compressions did not result in significantly improved results when compared to the results of the Flowtron. As such in this case the hypothesis that the added complexity of the "smart" timing would result in improved results over a similar device was not confirmed. Moreover, the "smart" timing of the CGC showed a more significant effect than that used within the SCD when in the seated position. As such the "smart" timing based on the cardiac gating proved to be more effective than the "smart" timing based on the vascular refill time.

Going forward it would be valuable to collect several physiological measures to better understand the impact of application of the IPC devices. Additionally, while this study determined the effect of the IPC devices on a healthy population it would be valuable to have further work done to compare the performance of the devices on patient groupings to determine the rate of DVT prevention.

Chapter 3

3.1 Introduction

Wearable sensors for physiological monitoring are becoming ever more prominent as medical and consumer products, enabling medical professionals and general consumers to track vitals continuously during activities of daily living. For clinical applications, they are being adopted to enable untethered monitoring of patients in the hospital and home care settings, thus affording a more complete record of a patient's health than can be obtained during a standard visit [68]–[71]. For both commercial and professional adoption, wearable sensors must be reliable, non-invasive, compact, and power efficient [41], [48], [68]–[71].

One of the most prevalent wearable sensor technologies is for heart rate monitoring, which is found in virtually all fitness monitors, due in part to the correlation between heart rate and physical exertion [20], [72]. Wearable heart rate monitors generally come in two classes: electrical pulse detection, similar to a traditional electrocardiogram (ECG); and photoplethysmography (PPG), an optical technology found in modern fitness and "smart" watches, as well as peripheral pulse detection sensors in clinical settings. PPG sensors are more convenient for integration into day-to-day life due to their small profile and cost in comparison to ECG based devices [47], [48]. PPG relies on a light source and photodetector pairing in order to illuminate the biological tissue and measure the variation in light intensity that results from the interaction between the light propagation and changes in blood volume under the probe [41]. Specifically, the AC component of the waveform contains information regarding the arterial blood volume changes in the area under the sensor, which corresponds to the person's cardiac cycle. The pulse rate is derived from

the peaks of the PPG waveform and has been shown to correspond to the R-R interval of an ECG waveform, demonstrating that this method can accurately measure heart rate [41]–[43].

PPG sensors typically have one of two configurations; transmittance- or reflectance-based sensors [41], [47], [73]. For transmittance-based sensors, the biological tissue is placed between the emitter and detector components, and thus the detector collects light that has passed completely through the tissue sample. This method is employed in thinner segments of the body, such as the fingers, ears, or toes [41], [47], [73], [74]. Reflectance-based sensors orient the emitter and detector components in approximately the same plane, which is then placed on the tissue of interest; the detector then collects light reflected back from the tissue sample. Because of the configuration, reflectance-based sensors can be used at more diverse measurement sites than transmission-based sensors. In clinical environments, transmittance-based sensors are typically employed due to their high accuracy; however, reflectance-based sensors are preferred for wearable sensor designs due to their versatility [75].

The skin tone of the user can affect performance of reflectance-based sensors [46], [76] by modulating the signal amplitude with minimal impact on the signal shape; therefore, it has been suggested that a higher intensity of light is required for darker skin tones in order to achieve the same signal strength and signal to noise ratio (SNR) with respect to physiological noise [46]. This suggests that the light intensity could be calibrated to achieve the optimal signal strength for a specific user and sensor location on the body [44], [74], [77]. However, calibration of PPG devices has primarily been done on light-skinned individuals, which results in poor performance on darker skin tones [50], [51]. Thus, a device's performance should be assessed on a wide range of skin tones to ensure that the quality of the pulse signal is adequate for all skin pigmentations. A pulse sensor with the capability to adjust the intensity of the light to maintain the signal integrity regardless of skin pigmentation would be beneficial for achieving the best sensor performance for a diverse population.

Optical pulse detection at peripheral locations, such as the upper and lower limb, has been demonstrated, particularly in non-motion conditions [44]–[46], [49]. Studies exploring lower limb detection have been limited to a single measurement site with no examination of optimized site selection based on signal strength or susceptibility to motion interference. Given differences in local vasculature and perfusion, it is expected that signal quality (strength and reflectance) will

vary with the selected measurement site [46], [49], [78]. It has been shown that different locations on the same subject's arm resulted in signals with different amplitudes [49], [78]. In addition, when testing with multi-channel PPG sensors, the configuration of the sensor's photodiode and red and infrared (IR) paired LEDs can affect the signal measured from the same location during movement [69], [79]. It remains to be investigated whether the signal acquisition could be improved during non-motion and motion conditions utilizing multiple LEDs and LED illumination configurations rather than the standard two LEDs fixed in position and paired to a photodiode.

A key performance metric for a wearable technology is battery life, as the device should be able to function continuously throughout the day. The LEDs used in wearables are one of the larger power drawing elements of the design [73]. There have been efforts attempting to develop low-power devices [70], [73]. Mendelson *et al*. (2006) noted that reducing the current drive to the LEDs would increase the battery life but sacrifice signal quality [73]. An increase in the number of detectors was proposed in order to mitigate the signal loss by capturing more back scattered light [73]. As an alternative, determination of the LED configuration resulting in a measurable PPG waveform at the lowest current requirement could improve sensor efficiency.

The objective of this manuscript is to develop a multi-LED PPG sensor and calibration scheme to extend battery life of a wearable heart rate monitor that is robust to location and skin pigmentation. In investigating application location, we consider the positional sensitivity to different types of movement to better facilitate the wearable nature of the sensor. Specific objectives to be addressed are: (i) test whether the calibration cycle can find the LED configuration for each individual that results in the highest pulse signal amplitude; (ii) determine if there is a location on the lower limb that allows for the LEDs to be at a lower intensity setting while still resulting in a reliable signal; and (iii) test the effect of movement of the lower limb on the signal captured by the sensor and if there exists a location on the lower limb where the pulse rate measurement is less susceptible to movement. These contributions can result in improved pulse sensor technology while providing information on the location on the lower limb that should be used for pulse rate measurements both at rest and during movement.

3.2 Sensor design

3.2.1 Sensor Layout

The customized sensor head, shown in Fig. 9, consists of 6 symmetrically spaced green LEDs (AA3528CGSK Kingbright, 574 nm peak wavelength, half-intensity angle ± 60˚) arranged in a ring. The peak wavelength of the LEDs falls within the range of wavelengths that has been shown to result in better detection of pulsatile blood volume changes across several skin tones (510 to 590 nm) within the range of visible and IR light (400 to 1000 nm) [46]. In addition, this wavelength was chosen as it has a shallower penetration depth into the tissue than red and IR light [46], [49], [76], [80], which results in the sensor's performance being less effected by the anatomical measurement site, as the underlying tissues and vessels attribute less noise in the reflected light [46], [49], [76], [80]. Cui *et al.* (1990) demonstrated that, in locations where there is a lower concentration of blood vessels, green light outperformed red light in returning a pulsatile signal [46]. Furthermore, it has been shown that reflectance pulse sensors that use green light are less sensitive to movement than red [81] and IR [49] based sensors.

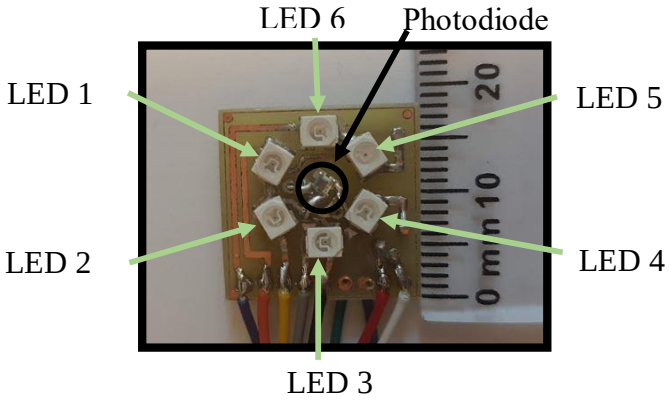

Fig. 9 Schematic of the sensor head. The sensor is 18 mm (vertical direction) by 18.5 mm (horizontal direction) with a thickness of 3.5 mm.

At the center of the LED ring is a single photodiode (PD) (APDS-9008 Avago Technologies, peak sensitivity wavelength 565 nm); the distance from the center of the PD to the center of each LED is 5 mm. The LEDs are symmetrically spaced around the PD at the chosen distance to maintain the AC component of the PPG waveform without the need for higher intensities; as it has been demonstrated that for a constant light intensity as the separation distance between the emitter

and detector is increased the signal amplitude of the detector will decrease exponentially [45]. The selected LED configuration also ensures that the proximity of the sources and detector does not result in the saturation of the photodiode with the DC component of the PPG waveform that results from the scattering of the emitted light in the upper blood-free layers of the skin [45]. Previous sensor studies have implemented a similar ring configuration, though the LEDs and PD positions were switched; that is, they comprised a ring of PDs surrounding two pairs of red and IR LEDs [79].

Each LED on the sensor head was assigned to a separate channel of a digital potentiometer (AD2506 Analog Devices, terminal resistance: 10kΩ) to enable independent control of the supply current, thus maximizing tunability. A DC current was supplied to the LEDs so that the luminous intensity emitted could be quantify based on the LED characteristics [82]. The LEDs chosen for this design have a linearly increasing relationship between the current drawn and the luminous intensity [82]. As such, a lower LED intensity should result in a longer battery life for the wearable sensor. The PD circuit isolates the frequencies of interest within the pulsatile signal using a combination of high and low pass filters with cut-off frequencies of 0.59 Hz and 3.32 Hz, respectively, which spans the frequency range of interest; this range corresponds to pulse rates between 35-199 bpm. The circuit removes the DC component of the pulse signal that is generated by the non-pulsatile surrounding tissue, venous blood, skin, and bone [41], [77], [83], and adds a reference voltage of 2.5V. A gain stage further increases the amplitude of the pulse signal. The PD chip itself contains a current to voltage converter, and thus additional external circuitry for this function was not required [84].

3.2.2 Calibration Cycle

The calibration cycle was developed such that, all permutations of the LEDs, from a single LED to all six illuminated simultaneously, are tested at three different intensity levels, leading to a total of 189 combinations. For each of the three intensity settings, the cumulative intensity of the illuminated LEDs was normalized to the number of LEDs lit in each permutation. That is, for a given intensity setting, the illumination intensity was the same, regardless of the number of illuminated LEDs. This enabled direct comparison of performance across all 63 LED illumination combinations. During testing, each LED combination was maintained for fourteen seconds; a seven second buffer was used to allow the signal time to settle after the change in configuration,

while the last seven seconds were used for data analysis. Each sensor head had a total calibration cycle time of 44.1 minutes for all three intensity levels and configuration permutations.

Each of the three sensors used in the study was consistently used in the same orientation and the same measurement location. As such should a trend appear in the pulse data collected which certain configurations it may be a result of the LEDs being brighter. However, while it could be intrinsic LED differences, preliminary testing was done to characterize the sensors' performance when removed from ambient light. The testing resulted in the average standard deviation around the average photodiode response to be within +/- 1.0% for each LED configuration across the three sensors when set to the lowest intensity used during the calibration cycle.

3.3 Experimental Methods

3.3.1 Protocols

The study was divided into three separate protocols. In all protocols, the participants were seated with their backs upright, knees at a 90˚ angle, and their lower legs perpendicular to the ground. The pulse signal was collected from three locations on the lower limb; the shin, the ankle, and the top of the foot, see Fig. 10. All participants were asked to remain still and refrain from speaking to reduce data contamination from noise and extraneous motion for the duration of the data collection.

The first protocol was designed to determine the lowest light intensity necessary for a measurable PPG waveform for two participants at the extremes of the considered skin pigmentation levels at each of the three lower limb measurement locations. The protocol was intended to aid in the identification of three target intensity levels (i.e. low, medium, and high) per measurement location, with the expectation that the low and high levels were representative of the intensity levels acceptable for the light and dark pigmentations, respectively. The medium light intensity level is the midpoint between the low and high setting. The three intensity levels determined within this pilot protocol were used in the subsequent calibration protocol. Two LEDs directly across from each other (LEDs 2 and 5, see Fig. 9) were illuminated on the sensor head and placed against the skin in each of the three measurement locations. This configuration was employed as it mimics the configurations employed in several commercial wearables, such as the Fitbit [85]. The intensities of the LEDs were systematically increased by stepping down the

resistance of the digital potentiometer by step sizes of 39 Ω while simultaneously recording the light returned to the PD. Each LED and intensity configuration was maintained for 11 seconds; a 4.5 second buffer was used to allow the signal to settle after the change in illumination intensity, while the last 6.5 seconds were used for data analysis. A smaller buffer was used for the pilot testing in comparison to the buffer size for the calibration cycle because pilot testing indicated that the resulting PPG signal was less impacted by the illumination intensity change of one step size in comparison to the modification of the LED configuration or larger illumination intensity changes, and thus required less settling time.

The second protocol used the calibration cycle in order to test if there exists an ideal LED illumination combination for maximizing the signal amplitude at the lowest intensity possible for a given user and measurement location. In the second protocol, the full calibration cycle was run on all participants with the intensities determined from the first protocol. The third protocol was designed to test the sensitivity of the sensor to motion at each measurement location. For this protocol, all six LEDs were illuminated at their highest intensity setting per location. Participants were asked to complete five different types of controlled movements, the order of which was randomized for each participant. Each of the five movements was performed at a frequency of 40 bpm (0.67 Hz) as indicated by a metronome. The five types of movement were: (1) ankle pivots (pivoting their foot at the ankle in the medial and lateral directions with the heel on the ground); (2) calf raises (keeping ball of the foot on the ground and lifting their heel); (3) foot flexes (lifting their foot upwards bending at the ankle while keeping their heel on the ground); (4) foot lifts (keeping their foot parallel to the ground and lifting their leg); (5) toe flexes (lifting their toes upward with their feet still resting on the floor).

The experimental protocol for this study received clearance from the University of Waterloo Research Ethics Committee (ORE #22756) and conformed to the Declaration of Helsinki.

3.3.2 Participants

Two healthy participants participated in the pilot intensity protocol, which were representative of the participants with the lightest and darkest skin pigmentation of all subsequent protocol participants. RGB values were measured on the lower leg for each participant to quantify

pigmentation levels; the lighter skin tone was measured as 200 172 153 and the darker skin tone was measured as 143 112 84.

Ten healthy participants (26.5 +/- 5.3 years old) were recruited for the calibration protocol. The average height and weight of the participants were 170.0 cm +/- 9.6 cm and 75.3 +/- 20.7 kg, respectively. The calibration protocol participants had varying skin pigmentations and self-identified their race, listed here in ascending order from lightest to darkest skin pigmentation: 4 Caucasians, 1 Asian, 3 South-East Asians, 1 South Asian, and 1 African-American.

For the motion protocol, ten healthy participants (26.5 +/- 5.3 years old) participated in the study with average height and weight of 171.0 cm +/- 10.1 cm and 76.8 +/- 22.2 kg, respectively. In ascending order from lightest to darkest skin pigmentation, participants were self-identified as: 5 Caucasians, 1 Asian, 2 South-East Asians, 1 South Asian, and 1 African-American.

3.3.3 Measurements

Three reflectance pulse sensors were used to simultaneously record the peripheral pulse rate from the shin, the ankle, and the top of the foot to enable monitoring of the circulation in the lower limb, see Fig. 10. These locations were chosen based on expected differences in the underlying physiology that will impact sensor pulse detection and movement artifacts in the signal waveform influenced by the range of motion at each location and relative distances to the leg joints. The sensor order was held consistent across participants; that is, the same sensor was always used for the ankle, etc.

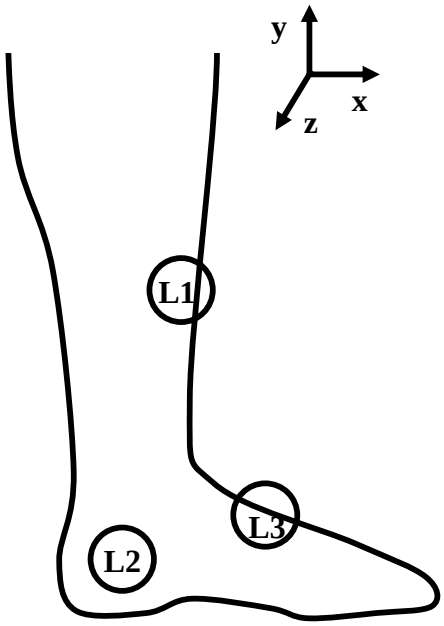

Fig. 10 The measurement locations on the left leg used in the study and coordinate system definition.

Anatomical landmarks and dimensions were used to place the sensors in a similar region across all participant's legs. The left leg was chosen as the measurement limb and was consistent across all participants. For the shin (L1) and ankle (L2), the sensors were taped in place such that LED 6 was at the highest superior position (y-direction, see Fig. 10). For the foot (L3), the sensor was taped in place such that LED 6 was the most medial (highest z value).

The three reflectance pulse sensors measured the pulse rate and a three-lead chest electrocardiogram (ECG) (Pilot 9200, Colin Medical Instruments Corp, San Antonio, Texas, USA) measured the heart rate. All measurements were concurrently acquired at 1 kHz using a Powerlab data acquisition system (Powerlab, ADInstruments, Colorado Springs, Colorado, USA) for comparison during each study protocol. For the intensity pilot protocol, a MM400 digital multimeter (MM400, Klein Tools, Inc., Lincolnshire, Illinois, USA) was used to measure the current supplied to each of the LEDs at each intensity setting tested. This current was converted to luminous intensity using the relationship provided on the datasheet for the LEDs.

3.3.4 Data Analysis

Data collected were filtered using a digital low pass filter to remove high frequency noise greater than 15 Hz. For the intensity pilot protocol (Protocol #1), the overall goal was to determine

the lowest intensity that resulted in the same amplitude of the pulse signal for each participant (skin tone) and location without performance errors. The amplitude (A) of each illumination configuration was considered as the average difference between the global maximum peak voltage (PV_{max}) and the global minimum peak voltage (PV_{min}) within the pulse signal per heartbeat,

$$A = \frac{\sum PV_{max} - \sum PV_{min}}{h_{pulse}} \quad [V] \quad (1)$$

where h_{pulse} is number of detected heartbeats in the analyzed PPG signal, see Fig. 11. The tolerance for equivalent amplitudes between the two participants was ± 0.004 V.

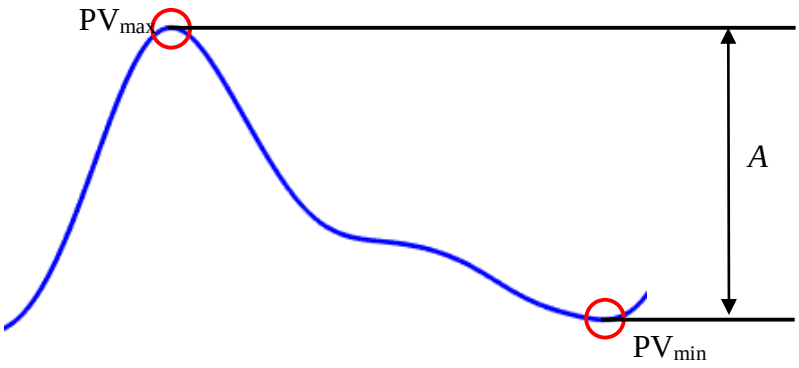

Fig. 11 Amplitude components of the PPG waveform for one heartbeat.

For a given illumination configuration, the performance error (PE) is defined as the difference between the number of heartbeats determined from the R peaks of the ECG waveform (h_{ecg}) and h_{pulse},

$$PE = |h_{ecg} - h_{pulse}| \quad (2)$$

The Matlab R2017b function `findpeaks` was used in order to capture the peaks of the ECG and PPG waveforms. The performance of the software was visually confirmed to be accurate by an observer for each measurement location per individual for all cases.

As discussed in Section 3.2.2, the illumination intensity was normalized such that it was nominally the same regardless of the number of LEDs in use for a given setting, low, medium, or high. The individual drive current for each LED within a specific LED configuration was identified at each cumulative target intensity level (i.e. low, medium, and high) to be used in the calibration

protocol. The tuned setting for each LED per target cumulative light intensity level was confirmed via repeated measures of the total light intensity at each LED configuration.

For the calibration protocol, the goal was to identify the LED illumination combination that resulted in the best signal, defined as the highest signal amplitude PPG waveform at the lowest intensity setting that did not incur performance errors, for each location and participant. The configurations that resulted in performance errors (Equation 2) were excluded from consideration when determining which signal had the highest amplitude (Equation 1).

Five different movements were tested with the sensors in place for the motion protocol. Motion artifact and the signal-to-noise ratios were used to quantify the sensor's pulse signal strength in comparison to that of the noise generated from the movements. The motion artifact ratio (AR) was taken as the average signal amplitude over 30s of movement (A_{mov}) divided by the average signal amplitude over 10s of rest data (A_{rest}) directly prior to movement [47], [49],

$$\mathrm{AR} = \frac{A_{\mathrm{mov}}}{A_{\mathrm{rest}}} \qquad (3)$$

The SNR was computed as the ratio between the maximum power within the pulse rate frequencies (P_{pr}) and the maximum power of the movement frequencies (P_{noise}) from the Fourier transformed signal, computed as

$$\mathrm{SNR} = 10\mathrm{Log}_{10}\left(\frac{\max\left(P_{\mathrm{pr}}\right)}{\max\left(P_{\mathrm{noise}}\right)}\right)\ [\mathrm{dB}] \qquad (4)$$

The range of frequencies of the movement was taken as the set movement frequency +/- 5% tolerance (0.63 - 0.7 Hz). The range of frequencies of the pulse rate was determined based on the ECG trace during movement, which was unaffected by the lower limb motion.

3.3.5 Statistical Analysis

Mixed effects models were employed to statistically compare the results from the motion protocol. The model considered each movement type and modelled the resulting motion artifact and the SNR based on the measurement locations as factors. These models contained three paired comparisons within the location factor. Hypothesis tests were performed using two-sided t-tests. Initially, the level of significance was set as $p<0.05$. However, in order to avoid Type I errors due

to multiple comparisons, the Bonferroni method was used to adjust the level of significance [62], which reduced it to $p<0.02$.

3.4 Results and Discussion

3.4.1 Intensity Setting with Varying Skin Tones

It has previously been shown that for a fixed green emission wavelength, the signal for a reflectance-based PPG was higher for light skin tones compared to darker skin tones [46], [76]. A similar skin tone-reflectance signal relationship was observed in this pilot, in which the intensity of the LEDs was consistently lower for the participant with a light skin tone for the same signal amplitude of both participants. The intensity settings of the light skin participant were used as the low intensity settings for the subsequent calibration protocol, while the intensity settings of the participant with the darker skin tone were used as the high intensity settings; this ensured that the calibration protocol would function for all explored skin tones. The medium intensity setting was chosen to be half-way between the low and high intensities. Table 7 shows the intensity values obtained in this study. Note that the medium intensity is not exactly halfway between low and high, but rather is the intensity setting that fell closest to this value; as the intensity values were constrained by the step size of the digital potentiometer.

Table 7: Calibration intensities resulting in the same amplitude across location and skin tone.

Measurement Location	Luminous Intensity Settings (mean +/- st. dev) [mcd]		
	Low	Medium	High
Foot	7.7 ± 0.1	14.4 ± 0.1	21.7 ± 0.3
Ankle	9.8 ± 0.1	68.1 ± 2.3	122.5 ± 5.0
Calf	14.4 ± 0.1	41.4 ± 0.3	68.1 ± 2.3

Each location required different intensity settings to result in the same amplitude of the pulse signal. This is consistent with signal amplitude differences across different measurement locations reported in prior research [49], [74], [78]. Both participants required the lowest luminous intensity at the foot measurement location. It is hypothesized that this is because the foot is more vascularized than the ankle or calf. This hypothesis is supported by the evidence that reflected PPG signals are typically greater in quality and magnitude when measured from areas of higher

vascularized areas with greater capillary densities [44]. The greater capillary density has been modelled to help the PPG amplitude as the transmural pressure from the arteries causes pulsatile modulations in the capillary beds thereby contributing to the PPG waveform [83]. Furthermore, it has been proven that most synovial joints have a high density capillary very superficially located [86]; and the foot measurement location is the only location located over planar synovial joints, as the shin site is located over the tibia and the ankle site is located over the calcaneus.

The participant with the dark skin pigmentation required a larger variation of intensities between locations than the participant with the light skin pigmentation. The differences in intensity for the participant with darker skin pigmentation could be attributed to different concentrations of melanin at the different sensor locations. Melanin effects the pigmentation of the skin, and has been proven to absorb large amounts of light emitted at shorter wavelengths [76]. The RGB values were only recorded at the shin as such difference concentrations could be present to impact the intensity required at each location. Another contributing factor could be the temperature of the skin and the effect on peripheral circulation. Cold temperatures have been shown to reduce the amplitude of PPG waveforms [80]. Attempts were made to control the room temperature where the testing occurred, however, skin temperature at the measurement location was not recorded. Therefore, it is possible the participant with dark skin pigmentation experienced vasoconstriction due to the localized temperature.

3.4.2 Calibration Cycle

An example of the pulse signals measured from each location at the high intensity, as well as the reference ECG trace is presented in Fig. 12. A DC offset and additional gain has been added to the pulse signals for plotting purposes. The R peak of the ECG and the peak of the PPG waveform denote the start of the systolic phase of the cardiac cycle [43]. Furthermore, the phase delay from the R peak of the ECG to the peak of the PPG waveform is the pulse wave transit time to the lower limb. The minor phase delay between the peripheral sensors measures the pulse transit time from the shin to the ankle and then to the foot. The three PPG signals are generally similar, exhibiting homologous cycle to cycle variations for most heartbeats.

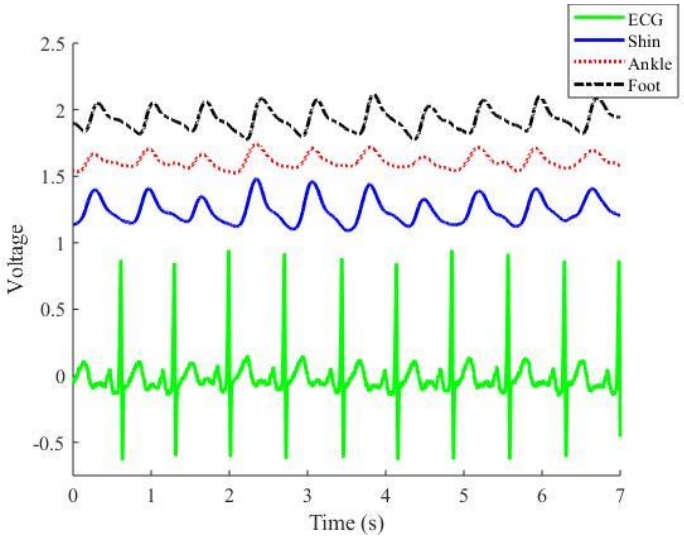

Fig. 12 Example PPG signals and corresponding ECG trace for one participant with additional gain and DC offsets.

Depending on the measurement site, different LED configurations were found to provide the best PPG signal, as defined in Section 3.3.4. For eight of the ten participants there was a configuration that resulted in a pulse signal that had no performance errors at the lowest of the three intensity settings, though the configuration generally differed somewhat between participants. The amplitude of two of the participants' foot signals steadily decayed over time. This is possibly due to a physiological response to remaining still for the length of the calibration cycle, resulting in perfusion changes in the lower limb. These two participants' foot signals were excluded from the summary of the results in Table 8, which indicates the LEDs illuminated (refer to Fig. 9 for the numbering convention) and minimum illumination setting that resulted in no performance errors; the participants are listed in order of ascending skin pigmentation.

Table 8: LED combination resulting in the best signal. Participants are listed in ascending order of skin pigmentation (i.e. participant 1 has the lightest pigmentation; participant 10 has the darkest).

Participant	Shin		Ankle		Foot	
	LEDs Illuminated	Intensity Setting	LEDs Illuminated	Intensity Setting	LEDs Illuminated	Intensity Setting
1	3,4,5	Low	3,4	Low	1,3,4	Low
2	5	Low	1,6	Low	1,2	Low
3	1,6	Low	2	Low	3	Low
4	1,2	Low	3	Low	---	---
5	6	Low	3	Low	1,2,5	Low
6	5	Low	1,2	Low	1	Low
7	5	Low	5	Low	---	---
8	1	Low	5	Medium	1	Medium
9	1	Low	2	Low	3	Low
10	6	Low	1,5	Medium	1	Low

The calibration cycle resulted in several trends with respect to the optimal LED configuration. The calibration cycle enabled the sensor to have the flexibility to find the illumination settings that worked best based on the underlying physiology; while the exact configurations vary, there was a visible trend toward illuminating LEDs from one side of the sensor resulting in the best signals at the shin and the foot locations. The side of the sensor that shows this trend was different in each of the locations, which suggests the performance difference may be due to the positioning and concentration of the blood vessels in those anatomical locations. Similarly, Lee *et al.* (2016) tested 21 locations in close proximity on the wrist and discovered significant differences in their measurements based on the capillaries and blood vessels under the measurement locations [78].

It is possible that the trends favouring one side of the sensor seen in Table 8 may be a result of the LEDs being brighter. Alternatively, it is hypothesized the tissue underneath the sensor encompasses the change in amplitude between the two sides of the sensor. As seen in the preliminary testing results discussed in Section 3.2.2, the photodiode response was similar across all configurations. Further preliminary testing was done to test all three sensors at the same measurement location on the shin to test if the best configuration that resulted followed the same trend of favouring one side seen in Table 8. While the configuration that produced the best signal

varied amongst the sensors, the trend continued of the best configuration including the LEDs from the upper half of the sensor (LEDs 1, 5 and 6, see Fig. 9) for all three sensors. The differences in the best configuration could be attributed to minor variation in the placement of the sensors as well as the contacting force used to secure the sensor in place, as the contacting force has been shown to have a significant impact on the PPG signal [87]. This lends credence to the hypothesis that the trend of one side of the sensor working better at the shin and foot is due to the underlying physiology rather than sensor bias. For the sensor on the foot it appears that more closely packed lateral and intermediate cuneiform bones is beneficial in comparison with the metatarsals for PPG measurement. Similarly, the sensor on the shin appears to be negatively affected by the tapering of the tibialis anterior muscle over the tibia in the sensor location.

Table 8 suggests that configurations with fewer LEDs illuminated tend to produce the best results. As discussed in Section 3.2.2, the illumination intensity was normalized such that it was nominally the same regardless of the number of LEDs in use for a given setting, low, medium, or high. As such, with more LEDs in use, the light was more diffuse, whereas fewer LEDs led to more intense localized light. Therefore it is hypothesized that having fewer LEDs illuminated at higher intensities in a localized region resulted in greater reflectance from the underlying vasculature when compared to the more diffuse illumination of many LEDs. More specifically, diffuse illumination led to an increased DC component of the signal, which obscured the pulsatile portion of the signal. The Beer-Lambert law states that the intensity of the light decreases exponentially as the penetration depth increases when in an absorbing medium [68]. We postulate that more diffuse light conditions resulted in a similar effect to lower intensity conditions, causing the emitted light to scatter on the bloodless shallower levels of the skin. It has been shown that higher intensities of light result in higher amplitudes of the PPG waveform [77]; however, this result shows that the intensity of the light is more effective in improving the amplitude if applied in higher concentrations.

The amplitude of the pulse signal averaged across all configurations with the same number of LEDs lit for one participant is presented in Fig. 13. The averaged data elucidate the trend in the PPG signal amplitude as increasing numbers of LEDs are lit. The maximum and minimum amplitude based on the number of LEDs lit are also presented to show the range of potential values for the one participant. The calibration cycle at the highest intensity is displayed, as this intensity

results in all configurations being free of performance errors for the selected participant. One participant was used as not all participants had calibration cycles free of performance errors. Further, the trends exhibited for the sample participant were similar across the other participants.

The maximum amplitude was observed to generally decrease when greater than 1 LEDs were illuminated for all measurement location, with the exception of the ankle, which was relatively insensitive to the illumination condition. Fig. 13 also highlights the wide range of measured amplitudes for configurations with the same number of illuminated LEDs. Furthermore, at the shin and ankle locations, the average signal amplitude does not change significantly as the illuminated LEDs increases, however large changes are observed in the maximum amplitude. These results demonstrate the importance of the calibration cycle to find the configuration that results in the maximal amplitude, which can be significantly higher than another configuration with the same number of LEDs illuminated. These findings further support the benefit of multiple LEDs and independent control capability to maximize the signal captured by the sensor.

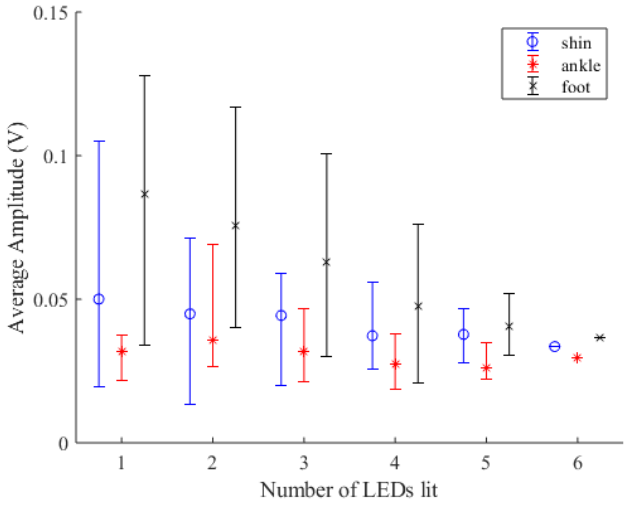

Fig. 13 Average, maximum, and minimum pulse signal amplitudes for the 6th participant based on the number of LEDs lit for each measurement location.

A measurable PPG signal was acquired for 8 of the 10 participants at the lowest intensity setting for all measurement locations, whereas the remainder of the participants (2 out of 10) required the medium intensity setting in at least one location. The participants requiring the medium intensity setting had darker skin tones, further supporting the need to calibrate sensor performance across a spectrum of skin tones due to performance differences [46], [50], [51], [76]. The adjustable

intensity settings allowed the sensor to adapt to different skin tones and to conserve battery life by increasing the intensity only to levels required for the best signal acquisition.

All of the configurations that required the medium setting were on the ankle or foot. However, while the shin does not require the medium settings, its low intensity setting does have the same power requirements as the foot's medium setting, as seen in Table 7. As such it holds no benefit to go with the shin over the foot with respect to power consumption. However, both the shin and the foot would be beneficial in comparison to the ankle in terms of allowing the use of intensity configurations with less power consumption.

3.4.3 Movement Effects

The motion protocol compared the sensor response at all locations to each of the five movements described in Section 3.3.1. The motion response was quantified by the motion artifact (Equation 3) and the signal to noise ratio (Equation 4). Within the results of the motion artifact it is preferable to have a lower motion artifact, as this indicates that the amplitude during movement is not altered from that during the rest condition. However, with the results of the signal to noise ratio, it is preferable to have a higher result as this indicates that the heart rate frequency contained by the pulse signal has not been obscured by the frequency of movement. The results of the motion protocol are presented in Fig. 14.

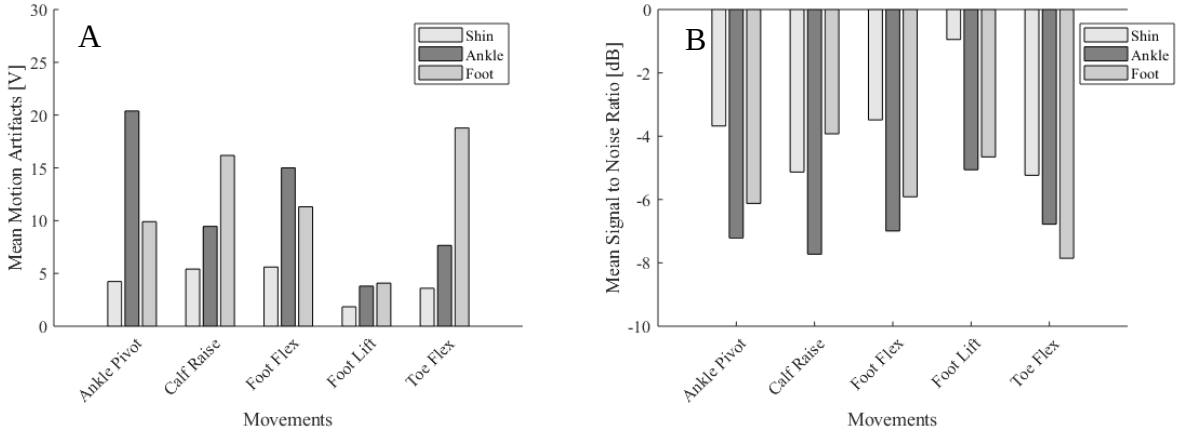

Fig. 14 Average movement response of the sensor at each location for all movement types (A – Motion artifact; B – Signal to noise ratio).

Within the ankle pivoting and the foot flex movements, the shin had a statistically ($p<0.02$) lower motion artifact and trends ($p<0.1$) towards a higher signal to noise ratio than the ankle, which

is unsurprising given the relatively mild shin movement in this region for such motions. The calf raise resulted in the shin having a statistically ($p<0.02$) lower motion artifact than the foot, similarly within the toe flex movement, the ankle and shin had statistically ($p<0.02$) lower motion artifacts than the foot, which is expected as the extensor digitorum longus muscle involved in these movements runs underneath the sensor location on the foot. The ankle pivoting movement resulted in the foot having statistically ($p<0.02$) lower motion artifacts than the ankle, which is somewhat surprising, given the greater acceleration experienced at the foot location for this motion however is likely due to the measurement location of the ankle as the location does constrict and stretch with the pivoting movement. The variance in the results suggest that the ankle and foot signals' resistance to motion are dependant on the type of movement.

Within each of the five types of movement tested, the shin had the lowest motion artifact overall. The SNR for the shin was also on average higher than the response of the other locations. This implies that the shin measurement location is more resistant to movement than the ankle or foot. Furthermore, this suggests that while the movement does affect the amplitude of the signal, the pulse frequency is not completely obscured during the movement when measuring from the shin. The shin having a lower motion artifact can be attributed to this location being furthest and therefore less affected by the majority of the joints and muscles manipulating the movements in the cases tested. Additionally, it has been shown that measurement locations on the peripheral sites of the arms, fingers and palms, have greater motion artifacts than those further from the periphery, this was attributed to the increased vasculature in the periphery resulting in greater blood volume changes during movement [49]. Based on the results of the study the increased motion artifacts found in the ankle and foot may be due to a higher number of vessels in the measurement location coupled with the increased proximity to the origins of several of the movements in comparison to the shin.

3.4.4 Limitations

The order in which the configurations were tested was consistent across all participants. Based on the duration of the calibration cycle it is possible that minor perfusion changes occurred that may have impacted which configuration was deemed best. Furthermore, the skin temperature at the sensor locations was not recorded so as to determine if the skin temperature played a role, through vasoconstriction with cold or vasodilation with heat, in determining the configuration with

the strongest amplitude. Finally, the sensors were only tested on the left leg of all participants and whether limb dominance would affect the results of the calibration cycle was not tested.

3.5 Conclusions

This study showed that the calibration cycle could be used to identify the LED configuration that maximized the pulse amplitude for each individual and measurement location at the lowest LED intensity setting without compromising sensor performance. As such the calibration cycle could potentially improve the battery life for each individual and measurement location without compromising the performance across different skin tones. Overall, the light intensities required to acquire the PPG waveform at the foot and the shin measurement locations resulted in the lowest power draw. However, the shin location was the most resistant to movement of the three locations. The motion conditions tested resulted in artifacts that overpowered the physiological signal for a subset of the test. However, the PPG waveform was still visible for several trials suggesting the potential to capture the pulse signal during certain motion conditions.

Multi-channel sensors with the ability to switch between individual PD channels have been shown to have certain channels be more resistant to motion artifacts in the pulse signal [69], [79]. As such future work should be done to test the calibration cycle during movement to see if there is a LED configuration that is more resistant to movement. Positional changes will result in perfusion changes in the sensor sites, the calibration cycle should therefore be tested in multiple positions to see if the ideal configuration shifts with posture. Additional testing should be done to determine if the calibration cycle will need to adjust the best configuration periodically as the sensor is worn over an extended period of time. As the shin location was the most resistant to movement, further testing could be done on the upper portion of the leg to see if the trend of moving further from the periphery continued to increase the sensor's resistance to movement.

Chapter 4

4.1 General Discussion

This thesis included two studies; one study examined the efficacy of the "smart" timing of a new IPC device built in-house in comparison to other commercial IPC devices with both fixed and "smart" timing of the compressions; the second study focused on the development and testing of a pulse sensor that could be integrated into the new IPC device to further improve its "smart" timing.

4.2 Summary of Findings

The first study compared the custom CGC device to other commercial devices to determine if one form of "smart" timing was more effective and if the devices which used "smart" timing resulted in significantly greater hemodynamic responses in comparison to the devices which used fixed timing. The custom IPC device used "smart" timing to apply compressions only during the diastolic phase of the cardiac cycle. This IPC device was compared to a device which used a similar rapid inflation, short duration profile but with fixed timing (VenaFlow), a device with a slow inflation, long duration compression profile (Flowtron), and a device which used a different form of "smart" timing to time compressions to the vascular refill time of the individual (SCD).

While seated, the CGC device resulted in significantly elevated muscle oxygenation, stroke volume, arterial velocity, and estimated venous blood displacement per hour in comparison to the commercial devices. This suggests that the CGC device was more efficient in returning venous blood to the heart and improving peripheral circulation. The added complexity of the "smart" timing for the CGC device was justified as it resulted in improved performance over a similar device which used fixed timing. However, the added complexity of the "smart" timing of the SCD

did not result in significantly different hemodynamic responses in comparison to the Flowtron which used fixed timing. Additionally, the “smart” timing used by the CGC device to compress rapidly during the diastolic phase of the cardiac cycle resulted in improved performance in comparison to the SCD which used “smart” timing to compress based on the vascular refill time, suggesting it is the better form of “smart” timing.

The second study was used to develop a pulse sensor that could be used as the timing method for the compressions of the CGC device. The pulse sensor was designed with a unique calibration cycle to test all possible LED configurations to determine the configuration that would maximize the amplitude of the signal per individual. This calibration cycle was tested across a broad range of skin tones, as previously performance errors have been found with optical technology on darker skin tones [50], [51]. The sensor was able to measure the pulse signal on all participants. Additionally, all participants resulted in different optimal configurations from the calibration cycle; with the majority of the configurations composed of one or two LEDs. This result suggests that going forward the calibration cycle need only alternate through LED configurations with up to two LEDs lit, thereby drastically decreasing the time of the cycle. Furthermore, the shin was determined to be the location on the lower limb that both allowed for a low luminous intensity setting to be used on all participants, while also being the location that was the most resistant to movement of the three locations (shin, ankle, foot) tested. There is potential for the sensor to be used on the shin to trigger compressions; ideally after undergoing the calibration cycle in order to use the strongest pulse signal for timing the compressions.

4.3 Thesis Limitations

Limitations of the research are based primarily on the sample population used in the research of this thesis.

The hemodynamic results seen with the CGC device are limited to the responses of a young, healthy population. While the results between healthy and patient populations will share similar trends in response to IPC devices, the hemodynamic responses have been found to be greater with healthy individuals in comparison to patient populations [7], [64]. Tests should be done to characterize the systemic and peripheral hemodynamic responses to the new IPC device in patient populations.

The pulse sensor was similarly limited to testing only on a young, healthy population. Prior research has shown that in low perfusion conditions the PPG technology is more susceptible to performance errors, particularly in darker skin tones [50], [51]. Furthermore, both age and illness can impact the shape of the PPG waveform [43], which may impact the peak detection used to determine the pulse arrival in the lower limb. Research should be done on patient populations with broad ranges of skin tones and ages to further characterize the performance of the pulse sensor.

4.4 Thesis Conclusions

In conclusion, the new IPC device that used "smart" timing to apply compressions during the diastolic phase of the cardiac cycle results in an increase in stroke volume, muscle oxygenation, peripheral arterial velocity and peripheral venous displacement over an hour period in comparison to other commercial IPC devices with both fixed and "smart" timing. The pulse sensor has been proven to work effectively on the lower limb and may be able to further improve the hemodynamic response of the device if used to time the compressions.

4.5 Future Work

The pulse sensor has been shown to accurately measure the pulse signal in the lower limb. However, as seen in this study and other research, a key source of performance errors with PPG sensors is their sensitivity to motion corruption [47]–[49], [69], [79], [81]. The sensor's sensitivity to motion may cause the sensor to be unreliable during the application of compressions, as the mechanical compressions will result in movement of the lower limb tissue. Additionally, because the noise generated from the compressions will be at the same frequency as the heart rate, due to the compressions being timed to the cardiac cycle, it will be much more difficult to isolate the pulse signal and filter out the noise. An investigation should be done to determine whether the pulse sensor can still accurately detect the pulse rate in the lower limb while compressions are taking place.

It may be beneficially to determine if placing the sensor further from the site of compressions on the calf could lower the impact of compressions on the signal quality. This is supported by the trends seen both in this study and other PPG research which shows that as the sensors are moved further from the periphery of the limb (fingers or toes) the signal is less contaminated by movement noise [49]. Despite it being likely that the thigh would require a higher luminous intensity setting

in order to capture the pulse signal, due to absorption of the light by adipose tissue, it may be more resistant to motion artifacts caused by compressions. Therefore, measurement sites on the thigh should be investigated as a potential sensor sites during use of the IPC device.

Another potential means of minimizing the effects of motion of the pulse signal would be to use multiple sensors. Previous use of multi-channel PPG sensors showed that the amount of motion corruption in the pulse signal of each channel during movement was different [69], [79]. As such it is possible that having multiple sensors could have a similar result and allow for the continuous determination of the sensor site with the best signal quality for the individual.

The pulse sensor was designed with the goal of replacing the current timing mechanism for the compressions of the custom IPC device. Should the pulse sensor be able to measure the pulse reliable during compressions then work should be done to allow communication between the pulse sensor and the compression triggering software. The peripheral and systemic hemodynamic responses to the current method of timing should be compared to the responses if the pulse sensor was used as the timing mechanism.

Pulse sensor could potentially be used as an assessment tool for local vasculature changes. As it is likely that vasculature conductance changes are occurring in the auxiliary vessels throughout compressions. Thereby the pulse sensor should be tested to see if it is able to detect the effectiveness of compressions as well as serve as a timing mechanism.

References

[1] A. Ruppert, T. Steinle, and M. Lees, "Economic burden of venous thromboembolism: a systematic review," *Journal of Medical Economics*, 2011.

[2] "Pulmonary Embolism (PE): Diagnosis," *Thrombosis Canada*, 2018. [Online]. Available: http://thrombosiscanada.ca/clinicalguides/?search=DVT#.

[3] A. L. Fogelson and K. B. Neeves, "Fluid Mechanics of Blood Clot Formation," *Annual Review of Fluid Mechanics*, vol. 47, no. 1, pp. 377–403, 2015.

[4] "Pulmonary Embolism (PE): Treatment," *Thrombosis Canada*, 2018. [Online]. Available: http://thrombosiscanada.ca/clinicalguides/?search=DVT#. [Accessed: 06-Sep-2018].

[5] S. M. Pastores, "Management of venous thromboembolism in the intensive care unit," *Journal of Critical Care*, vol. 24, no. 2, pp. 185–191, 2009.

[6] R. J. Morris and J. P. Woodcock, "Evidence-Based Compression," *Annals of Surgery*, vol. 239, no. 2, pp. 162–171, 2004.

[7] M. D. Malone, P. L. Cisek, J. Comerota, B. Holland, I. G. Eid, and A. J. Comerota, "High-pressure, rapid-inflation pneumatic compression improves venous hemodynamics in healthy volunteers and patients who are post-thrombotic," *Journal of Vascular Surgery*, vol. 29, no. 4, pp. 593–599, 1999.

[8] R. J. Morris, "Intermittent pneumatic compression-systems and applications," *Journal of medical engineering & technology*, vol. 32, no. 3, pp. 179–188, 2008.

[9] R. J. Morris, J. C. Giddings, H. M. Ralis, G. M. Jennings, D. A. Davies, J. P. Woodcock, and F. D. J. Dunstan, "The influence of inflation rate on the hematologic and hemodynamic effects of intermittent pneumatic calf compression for deep vein thrombosis prophylaxis," *Journal of Vascular Surgery*, vol. 44, no. 5, pp. 1039–1045, 2006.

[10] S. K. Kakkos, M. Griffin, G. Geroulakos, and A. N. Nicolaides, "The efficacy of a new portable sequential compression device (SCD Express) in preventing venous stasis," *Journal of Vascular Surgery*, vol. 42, no. 2, pp. 296–303, 2005.

[11] A. G. G. Turpie, T. Delmore, J. Hirsh, R. Hull, E. Genton, C. Hiscoe, and M. Gent, "Prevention of venous thrombosis by intermittent sequential calf compression in patients with intracranial disease," *Thrombosis Research*, vol. 15, no. 5–6, pp. 611–616, 1979.

[12] N. Labropoulos, J. Cunningham, S. S. Kang, M. A. Mansour, and W. H. Baker, "Optimising the performance of intermittent pneumatic compression devices," *EJVES Extra*, vol. 19, no. 6, pp. 593–597, 2010.

[13] E. A. Lachmann, J. L. Rook, R. Tunkel, W. Nagler, and W. N. Elisabeth A. Lachmann, Jack L. Rook, Richard Tunkel, "Complications associated with intermittent pneumatic compression devices," *the American Congress of Rehabilitation Medicine, and the American Academy of Physical Medicine and Rehabilitation*, vol. 93, no. 6, pp. 482–485, 1992.

[14] M. Borow and H. Goldson, “Postoperative venous thrombosis. Evaluation of five methods of treatment,” *The American Journal of Surgery*, vol. 141, no. 2, pp. 245–251, 1981.

[15] D. J. Warwick and K. Dewbury, “A novel approach to mechanical prophylaxis: Calf impulse technology mimics natural ambulation more effectively than sequential calf compression,” *International Journal of Angiology*, vol. 17, no. 4, pp. 197–202, 2008.

[16] R. Eisele, L. Kinzl, and T. Koelsch, “Rapid-inflation intermittent pneumatic compression for prevention of deep venous thrombosis.,” *The Journal of Bone and Joint Surgery. American Volume*, vol. 89, no. 5, pp. 1050–6, 2007.

[17] M. C. Proctor, L. J. Greenfield, T. W. Wakefield, and P. J. Zajkowski, “A clinical comparison of pneumatic compression devices: The basis for selection,” *Journal of Vascular Surgery*, vol. 34, no. 3, pp. 459–464, 2001.

[18] P. F. Lachiewicz, S. S. Kelley, and L. R. Haden, “Two mechanical devices for prophylaxis of thromboembolism after total knee arthroplasty. A prospective, randomised study.,” *The Journal of Bone and Joint Surgery. British Volume*, vol. 86, no. 8, pp. 1137–41, 2004.

[19] “Deep vein thrombosis (DVT): Diagnosis,” *Thrombosis Canada*, 2018. [Online]. Available: http://thrombosiscanada.ca/clinicalguides/?search=DVT#. [Accessed: 01-Aug-2018].

[20] D. U. Silverthorn, *Human Physiology: An Integrated Approach*, 5th ed. San Francisco: Pearson Education, Inc., 2010.

[21] K. T. Delis, N. Labropoulos, A. N. Nicolaides, B. Glenville, and G. Stansby, “Effect of intermittent pneumatic foot compression on popliteal artery haemodynamics,” *European Journal of Vascular and Endovascular Surgery*, vol. 19, no. 3, pp. 270–277, 2000.

[22] C.-C. Huang, S.-H. Wang, and P.-H. Tsui, “In Vitro Study on Assessment of Blood Coagulation and Clot Formation Using Doppler Ultrasound.,” *Japanese Journal of Applied Physics*, vol. 44, no. 12, pp. 8727–8732, 2005.

[23] N. Krasokha, W. Theisen, S. Reese, P. Mordasini, C. Brekenfeld, J. Gralla, J. Slotboom, G. Schrott, and H. Monstadt, “Mechanical properties of blood clots - A new test method,” *Materialwissenschaft und Werkstofftechnik*, vol. 41, no. 12, pp. 1019–1024, 2010.

[24] M. D. Malone, P. L. Cisek, A. J. Comerota Jr, B. Holland, I. G. Eid, and A. J. Comerota, “High-pressure, rapid-inflation pneumatic compression improves venous hemodynamics in healthy volunteers and patients who are post-thrombotic.,” *Journal of Vascular Surgery*, vol. 29, no. 4, pp. 593–599, 1999.

[25] R. J. Morris and J. P. Woodcock, “Intermittent venous compression, and the duration of hyperaemia in the common femoral artery,” *Clinical Physiology and Functional Imaging*, 2004.

[26] J. Book, C. N. Prince, R. Villar, R. L. Hughson, and S. D. Peterson, “Investigating the impact of passive external lower limb compression on central and peripheral hemodynamics during exercise,” *European Journal of Applied Physiology*, vol. 116, no. 4, pp. 717–727, 2016.

[27] K. T. Delis and A. L. Knaggs, “Duration and amplitude decay of acute arterial leg inflow enhancement with intermittent pneumatic leg compression: An insight into the implicated physiologic mechanisms,” *Journal of Vascular Surgery*, vol. 42, no. 4, pp. 717–725, 2005.

[28] K. T. Delis, Z. A. Azizi, R. J. G. Stevens, J. H. N. Wolfe, and A. N. Nicolaides, “Optimum intermittent pneumatic compression stimulus for lower-limb venous emptying,” *European Journal of Vascular and Endovascular Surgery*, vol. 19, no. 3, pp. 261–269, 2000.

[29] M. Helmi, D. Gommers, and A. B. J. Groeneveld, “A review of the hemodynamic effects of external leg and lower body compression,” *Minerva Anestesiologica*, vol. 80, no. 3, pp. 355–365, 2014.

[30] K. T. Delis, M. J. Husmann, N. J. Cheshire, and a N. Nicolaides, “Effects of intermittent pneumatic compression of the calf and thigh on arterial calf inflow: a study of normals, claudicants, and grafted arteriopaths.,” *Surgery*, vol. 129, no. 2, pp. 188–195, 2001.

[31] R. Kamm, R. Butcher, J. Froelich, M. Johnson, E. Salzman, A. Shapiro, and H. W. Strauss, “Optimisation of indices of external pneumatic compression for prophylaxis against deep vein thrombosis: Radionuclide gated imaging studies,” *Cardiovascular Research*, vol. 20, no. 8, pp. 588–596, 1986.

[32] F. Lurie, D. J. Awaya, R. L. Kistner, and B. Eklof, “Hemodynamic effect of intermittent pneumatic compression and the position of the body,” *Journal of Vascular Surgery*, vol. 37, no. 1, pp. 137–142, 2003.

[33] R. H. Morgan, G. Carolan, J. V. Psaila, a. M. N. Gardner, R. H. Fox, and J. P. Woodcock, “Arterial Flow Enhancement by Impulse Compression,” *Vascular and Endovascular Surgery*, vol. 25, no. 1, pp. 8–16, 1991.

[34] “Flowtron ACS800 + Tri Pulse: Instructions for Use.” ArjoHuntleigh, Malmö, pp. 1–40, 2014.

[35] “The Flowtron Active Compression System: Tri Pulse Garment and ACS800 Pump.” ArjoHuntleigh, Malmö, pp. 1–6, 2014.

[36] M. Griffin, S. K. Kakkos, G. Geroulakos, and A. N. Nicolaides, “Comparison of Three Intermittent Pneumatic Compression Systems in Patients in Patients with Varicose Veins: A Hemodynamic Study,” *International Angiology*, no. 5, 2007.

[37] S. K. Kakkos, A. N. Nicolaides, M. Griffin, and G. Geroulakos, “Comparison of two intermittent pneumatic compression systems. A hemodynamic study,” *International Angiology*, vol. 24, no. 4, pp. 330–335, 2005.

[38] M. Griffin, S. K. Kakkos, G. Geroulakos, and A. N. Nicolaides, “Comparison of efficacy of the intermittent pneumatic compression,” *International Angiology*, 2005.

[39] O. Tochikubo, S. Ri, and N. Kura, “Effects of pulse-synchronized massage with air cuffs on peripheral blood flow and autonomic nervous system,” *Circulation Journal*, vol. 70, no. 9, pp. 1159–1163, 2006.

[40] K. A. Zuj, C. N. Prince, R. L. Hughson, and S. D. Peterson, “Enhanced muscle blood flow

with intermittent pneumatic compression of the lower leg during plantar flexion exercise and recovery.," *Journal of Applied Physiology*, p. jap.00784.2017, 2017.

[41] J. Allen, "Photoplethysmography and its application in clinical physiological measurement," *Physiological Measurement*, vol. 28, no. 3, 2007.

[42] A. Reisner, P. A. Shaltis, D. McCombie, and H. H. Asada, "Utility of the Photoplethysmogram in Circulatory Monitoring," *Anesthesiology*, vol. 108, no. 5, pp. 950–958, 2008.

[43] M. Elgendi, "On the Analysis of Fingertip Photoplethysmogram Signals," *Current Cardiology Reviews*, vol. 8, no. 1, pp. 14–25, 2012.

[44] Y. Mendelson and M. J. McGinn, "Skin reflectance pulse oximetry: in vivo measurements from the forearm and calf.," *Journal of clinical monitoring*, 1991.

[45] Y. Mendelson and B. D. Ochs, "Noninvasive Pulse Oximetry Utilizing Skin Reflectance Photoplethysmography," *IEEE Transactions on Biomedical Engineering*, vol. 35, no. 10, pp. 798–805, 1988.

[46] W. Cui, L. E. Ostrander, and B. Y. Lee, "In vivo reflectance of blood and tissue as a function of light wavelength," *IEEE Transactions on Biomedical Engineering*, vol. 37, no. 6, pp. 632–639, 1990.

[47] C. Zhou, J. Feng, J. Hu, and X. Ye, "Study of Artifact-Resistive Technology Based on a Novel Dual Photoplethysmography Method for Wearable Pulse Rate Monitors," *Journal of medical systems*, vol. 40, no. 3, p. 56, 2016.

[48] S. M. A. Salehizadeh, D. Dao, J. Bolkhovsky, C. Cho, Y. Mendelson, and K. H. Chon, "A novel time-varying spectral filtering algorithm for reconstruction of motion artifact corrupted heart rate signals during intense physical activities using a wearable photoplethysmogram sensor," *Sensors (Switzerland)*, vol. 16, no. 1, 2015.

[49] Y. Maeda, M. Sekine, and T. Tamura, "Relationship between measurement site and motion artifacts in wearable reflected photoplethysmography," *Journal of Medical Systems*, vol. 35, no. 5, pp. 969–976, 2011.

[50] P. E. Bickler, J. R. Feiner, and J. W. Severinghaus, "Effects of skin pigmentation on pulse oximeter accuracy at low saturation," *Anesthesiology*, 2005.

[51] J. R. Feiner, J. W. Severinghaus, and P. E. Bickler, "Dark skin decreases the accuracy of pulse oximeters at low oxygen saturation: The effects of oximeter probe type and gender," *Anesthesia and Analgesia*, 2007.

[52] S. Nomura, Y. Hanasaka, M. Hasegawa-Ohira, T. Ishiguro, and H. Ogawa, "Identification of human pulse waveform by silicon microphone chip," in *Conference Proceedings - IEEE International Conference on Systems, Man and Cybernetics*, 2011, pp. 1145–1150.

[53] V. Goverdovsky, D. Looney, P. Kidmose, C. Papavassiliou, and D. P. Mandic, "Co-located multimodal sensing: A robust solution for next generation wearable health," *IEEE Sensors Journal*, vol. 15, no. 1, pp. 138–145, 2015.

[54] D. G. Jakovljevic, M. I. Trenell, and G. A. MacGowan, “Bioimpedance and bioreactance methods for monitoring cardiac output,” *Best Practice and Research: Clinical Anaesthesiology*, vol. 28, no. 4, pp. 381–394, 2014.

[55] M.-C. Cho, J.-Y. Kim, and S.-H. Cho, “A bio-impedance measurement system for portable monitoring of heart rate and pulse wave velocity using small body area,” *2009 IEEE International Symposium on Circuits and Systems*, vol. 1, pp. 3106–3109, 2009.

[56] R. H. Morgan, G. Carolan, J. V. Psaila, A. M. N. Gardner, R. H. Fox, and J. P. Woodcock, “Arterial Flow Enhancement by Impulse Compression,” *Vascular and Endovascular Surgery*, 1991.

[57] M. Griffin, S. K. Kakkos, G. Geroulakos, and A. N. Nicolaides, “Comparison of three intermittent pneumatic compression systems in patients with varicose veins: A hemodynamic study,” *International Angiology*, vol. 26, no. 2, pp. 158–164, 2007.

[58] R. D. Kamm, “Bioengineering studies of periodic external compression as prophylaxis against deep vein thrombosis-part I: numerical studies,” *Journal of Biomechanical Engineering*, vol. 104, no. 2, pp. 87–95, 1982.

[59] D. A. Olson, R. D. Kamm, and A. H. Shapiro, “Bioengineering studies of periodic external compression as prophylaxis against deep vein thrombosis-part II: experimental studies on a stimulated leg.,” *Journal of Biomechanical Engineering*, vol. 104, no. 2, pp. 96–104, 1982.

[60] K. T. Delis, Z. A. Azizi, R. J. G. Stevens, J. H. N. Wolfe, and A. N. Nicolaides, “Optimum intermittent pneumatic compression stimulus for lower-limb venous emptying,” *European Journal of Vascular and Endovascular Surgery*, vol. 19, no. 3, pp. 261–269, 2000.

[61] I. Diamantopoulos and M. J. Lever, “Can an intermittent pneumatic compression system monitor venous filling in the leg?,” *Journal of Medical Engineering and Technology*, vol. 32, no. 3, pp. 221–7, 2008.

[62] S. Kuiper and J. Sklar, “Practicing Statistics: Guided Investigations for the Second Course,” *Pearson Education*. p. 21, 2013.

[63] A. Bickel, A. Shturman, I. Grevtzev, N. Roguin, and A. Eitan, “The physiological impact of intermittent sequential pneumatic compression (ISPC) leg sleeves on cardiac activity,” *American Journal of Surgery*, vol. 202, no. 1, pp. 16–22, 2011.

[64] A. R. Eze, A. J. Comerota, P. L. Cisek, B. S. Holland, R. P. Kerr, R. Veeramasuneni, and A. J. Comerota Jr, “Intermittent calf and foot compression increases lower extremity blood flow,” *American Journal of Surgery*, vol. 172, no. 2, pp. 130–135, 1996.

[65] A. H. Chen, S. G. Frangos, S. Kilaru, and B. E. Sumpio, “Intermittent pneumatic compression devices - Physiological mechanisms of action,” *European Journal of Vascular and Endovascular Surgery*, vol. 21, no. 5, pp. 383–392, 2001.

[66] A. J. Comerota, “Intermittent pneumatic compression: Physiologic and clinical basis to improve management of venous leg ulcers,” *Journal of Vascular Surgery*, vol. 53, no. 4, pp. 1121–1129, 2011.

[67] F. Lurie, V. Scott, H. C. Yoon, and R. L. Kistner, "On the mechanism of action of pneumatic compression devices: Combined magnetic resonance imaging and duplex ultrasound investigation," *Journal of Vascular Surgery*, vol. 48, no. 4, pp. 1000–1006, 2008.

[68] J. Wannenburg and R. Malekian, "Body Sensor Network for Mobile Health Monitoring, a Diagnosis and Anticipating System," *IEEE Sensors Journal*, vol. 15, no. 12, pp. 6839–6852, 2015.

[69] Y. Mendelson, D. K. Dao, and K. H. Chon, "Multi-channel pulse oximetry for wearable physiological monitoring," *2013 IEEE International Conference on Body Sensor Networks, BSN 2013*, 2013.

[70] S. J. Jung, Y. D. Lee, Y. S. Seo, and W. Y. Chung, "Design of a low-power consumption wearable reflectance pulse oximetry for ubiquitous healthcare system," *2008 International Conference on Control, Automation and Systems, ICCAS 2008*, pp. 526–528, 2008.

[71] R. G. Haahr, S. B. Duun, M. H. Toft, B. Belhage, J. Larsen, K. Birkelund, and E. V. Thomsen, "An electronic patch for wearable health monitoring by reflectance pulse oximetry," *IEEE Transactions on Biomedical Circuits and Systems*, vol. 6, no. 1, pp. 45–53, 2012.

[72] N. Kakarot and F. Müller, "Assessment of physical strain in younger and older subjects using heart rate and scalings of perceived exertion," *Ergonomics*, vol. 57, no. 7, pp. 1052–1067, 2014.

[73] Y. Mendelson, R. J. Duckworth, and G. Comtois, "A wearable reflectance pulse oximeter for remote physiological monitoring," *Annual International Conference of the IEEE Engineering in Medicine and Biology - Proceedings*, pp. 912–915, 2006.

[74] M. Nogawa, T. Kaiwa, and S. Takatani, "A novel hybrid reflectance pulse oximeter sensor with improved linearity and general applicability to various portions of the body," *Proceedings of the 20th Annual International Conference of the IEEE Engineering in Medicine and Biology Society. Vol.20 Biomedical Engineering Towards the Year 2000 and Beyond (Cat. No.98CH36286)*, vol. 4, no. 4, pp. 1858–1861, 1998.

[75] H. Lee, H. Ko, and J. Lee, "Reflectance pulse oximetry: Practical issues and limitations," *ICT Express*, 2016.

[76] R. R. Anderson and J. A. Parrish, "The Optics of Human Skin," *Journal of Investigative Dermatology*, vol. 77, no. 1, pp. 13–19, 1981.

[77] R. Shriram, M. Sundhararajan, and N. Daimiwal, "Effect of change in intensity of infrared LED on a photoplethysmogram," *International Conference on Communication and Signal Processing, ICCSP 2014 - Proceedings*, pp. 1064–1067, 2014.

[78] S. Lee, H. Shin, and C. Hahm, "Effective PPG sensor placement for reflected red and green light, and infrared wristband-type photoplethysmography," *International Conference on Advanced Communication Technology, ICACT*, vol. 2016–March, pp. 556–558, 2016.

[79] K. M. Warren, J. R. Harvey, K. H. Chon, and Y. Mendelson, "Improving pulse rate

measurements during random motion using a wearable multichannel reflectance photoplethysmograph," *Sensors (Switzerland)*, vol. 16, no. 3, 2016.

[80] Y. Maeda, M. Sekine, and T. Tamura, "The advantages of wearable green reflected photoplethysmography," *Journal of Medical Systems*, vol. 35, no. 5, pp. 829–834, 2010.

[81] J. Lee, K. Matsumura, K. Yamakoshi, P. Rolfe, S. Tanaka, and T. Yamakoshi, "Comparison between red, green and blue light reflection photoplethysmography for heart rate monitoring during motion.," *35th Annual International Conference of the IEEE Engineering in Medicine and Biology Society (EMBC)*, pp. 1724–1727, 2013.

[82] C. H. Han, "Kingbright: AA3528CGSK." Kingbright, pp. 1–4, 2012.

[83] A. A. Kamshilin and N. B. Margaryants, "Origin of Photoplethysmographic Waveform at Green Light," in *Physics Procedia*, 2017.

[84] Avago, "APDS-9008: Miniature Surface-Mount Ambient Light Photo Sensor." Avago Technologies, pp. 1–12, 2008.

[85] "PurePulse Technology," *Fitbit INC.*, 2018. [Online]. Available: https://www.fitbit.com/en-ca/purepulse. [Accessed: 22-Aug-2018].

[86] A. D. Knight and J. R. Levick, "The Density and Distribution of Capillaries around a Cynovial Cavity," *Quarterly Journal of Experimental Physiology*, no. 68, pp. 629–644, 1983.

[87] X. F. Teng and Y. T. Zhang, "The effect of contacting force on photoplethysmographic signals," *Physiological Measurement*, vol. 25, no. 5, pp. 1323–1335, 2004.